AD/A-003 835

MACHINE CASTING OF FERROUS ALLOYS

M. F. X. Gigliotti, Jr.

General Electric Corporate Research and Development

Prepared for:

Army Materials and Mechanics Research Center
Advanced Research Projects Agency

October 1974

UNCLASSIFIED

SECURITY CLASSIFICATION OF THIS PAGE *(When Data Entered)*

REPORT DOCUMENTATION PAGE		READ INSTRUCTIONS BEFORE COMPLETING FORM
1. REPORT NUMBER AMMRC CTR 74-65	2. GOVT ACCESSION NO.	3. RECIPIENT'S CATALOG NUMBER AD/A-003835
4. TITLE *(and Subtitle)* Machine Casting of Ferrous Alloys		5. TYPE OF REPORT & PERIOD COVERED Final Report Feb. 1, 1973 to June 30, 1974
		6. PERFORMING ORG. REPORT NUMBER SRD-74-079
7. AUTHOR(s) M. F. X. Gigliotti, Jr.		8. CONTRACT OR GRANT NUMBER(s) DAAG46-73-C-0111
9. PERFORMING ORGANIZATION NAME AND ADDRESS Corporate Research and Development General Electric Company Schenectady, New York 12301		10. PROGRAM ELEMENT, PROJECT, TASK AREA & WORK UNIT NUMBERS ARPA Order No. 2267 AMCMS Code 4D10 Agency Acc. No: DAOE 4736
11. CONTROLLING OFFICE NAME AND ADDRESS Army Materials and Mechanics Research Center Watertown, Massachusetts 02172		12. REPORT DATE October 1974 13. NUMBER OF PAGES 92
14. MONITORING AGENCY NAME & ADDRESS*(If different from Controlling Office)*		15. SECURITY CLASS. *(of this report)* Unclassified 15a. DECLASSIFICATION/DOWNGRADING SCHEDULE

16. DISTRIBUTION STATEMENT *(of this Report)*

Approved for public release; distribution unlimited.

17. DISTRIBUTION STATEMENT *(of the abstract entered in Block 20, if different from Report)*

18. SUPPLEMENTARY NOTES

19. KEY WORDS *(Continue on reverse side if necessary and identify by block number)*

ferrous die casting, rheocasting, solidification

20. ABSTRACT *(Continue on reverse side if necessary and identify by block number)*

A series of iron, nickel, and cobalt base alloys have been permanent mold cast under varying conditions to evaluate techniques for improving the integrity of die castings. By appropriate control of heat flow, it is possible to achieve permanent mold casting with mechanical properties equivalent to investment castings. Liquid-solid slurries were cast (Rheocasting) to evaluate casting properties and opportunities for enhanced mold life with a reduced temperature casting process. Casting properties are acceptable. It is not clear that there

DD FORM 1 JAN 73 1473 EDITION OF 1 NOV 65 IS OBSOLETE

UNCLASSIFIED

SECURITY CLASSIFICATION OF THIS PAGE *(When Data Entered)*

is enhanced mold life by this process. Stainless steel alloys were die cast at 34 - 105°C superheats. These die castings indicate that there is sufficient heat loss in the shot sleeve and runner systems that the metal arrives in the die cavity partly solid.

AMMRC CTR 74-65

MACHINE CASTING OF FERROUS ALLOYS

OCTOBER 1974

M. F. X. Gigliotti, Jr.
CORPORATE RESEARCH AND DEVELOPMENT
GENERAL ELECTRIC COMPANY
SCHENECTADY, NEW YORK 12301
(518) 346-8771, Ext. 6586

FINAL TECHNICAL REPORT CONTRACT No. DAAG 46-73-C-0111

Sponsored by: Advanced Research Projects Agency, ARPA Order No. 2267, Amendment #2

Program Code No. 4D10

Effective Date of Contract: February 1, 1973

Contract Expiration Date: August 30, 1974

Amount of Contract $223,010

Contract Period Covered by Report: 01 February 1973 - 30 June 1974

Prepared for:

ARMY MATERIALS AND MECHANICS RESEARCH CENTER
Watertown, Massachusetts 02172

LIST OF ILLUSTRATIONS

Figure 18 Same casting as Fig. 17. Center of web section. Coarser structure than Fig. 17. Marble's reagent. 250X

Figure 19 TRW VI A cast in permanent mold at 1430°C and 400°C mold temp. Center of thick section of casting. Ni-base dendrites surrounded by network of γ-γ' eutectic. Porosity associated with eutectic in lower center. Marble's reagent. 250X

Figure 20 TRW VI A casting same as Fig. 19. Center of web section. Same features as thick section except coarser microstructure. Porosity associated with γ-γ' eutectic in lower right. Marble's reagent. 250X

Figure 21 TRW VI A casting same as Figs. 19 and 20. Microporosity associated with γ-γ' eutectic. Marble's reagent. 250X

Figure 22 Blade shape mold machined from block of ZRBSC-M(R). Mold has cracks in root section which occurred during pouring.

Figure 23 Blade mold with alumina insert tubes. Cracks repaired with powdered graphite and potassium silicate.

Figure 24 Mar M 302 blade shape casting. Poured at 1430°C, 550°C mold temperature. Ceramic tube removed.

Figure 25 Cross sections of casting shown in Fig. 24. No gross porosity visible. Upper section is midplane of root section. Lower section is midplane through blade. Riser not shown.

Figure 26 Microstructure of blade casting shown in Fig. 24. Structure is finer than that in Figs. 17 and 18. No porosity evident. Marble's reagent. 250X

TABLE OF CONTENTS

I. INTRODUCTION AND SUMMARY

To apply an automated machine casting process which uses reusable metal molds to structural castings of materials, a central problem to be overcome is the lack of soundness associated with die castings. This lack of soundness is due to both solidification shrinkage and to entrainment of gas during injection of metal into the mold.[1]

The general purpose of this work was to identify techniques which will produce sound castings in reusable chill molds, - which techniques are compatible with an automated machine casting process.

To do this, we studied castings made in permanent chill molds, initially divorced from any consideration of the type of machine which would produce such castings, since the use of an automated process for structural materials depends on the casting's integrity. The automated machine will have to fit the process.

Initial work indicated that ceramic inserts markedly improve the soundness of chill castings. Inserts are used to direct heat flow to allow feeding of the casting. Inserts are also used to reduce hot tearing and cracking due to mold-casting mechanical interactions.

Casting integrity is also a sensitive function of alloy type. Castings with long freezing ranges have large amounts of microporosity, while those with short freezing ranges have little. Mechanical testing confirms this difference with a chill-cast, short-freezing-range alloy having comparable stress rupture behavior to the investment cast alloy, while a long-freezing range alloy has degraded properties.

Rheocasting (casting of liquid-solid slurries) has been extended to stainless steels and super-alloys. Properties of rheocast material are equivalent to conventionally cast. Measurements of mold temperature response during casting indicate that the mold face temperature rise is essentially the same for rheocasting and conventional casting. Further, metallography of ferrous die castings indicates that the metal loses sufficient heat in the shot sleeve and runner system that it has begun solidifying before it arrives in the mold cavity. It is thus not clear that rheo-die casting has any advantages over the presently developed ferrous die casting process.

In summary, this work concludes:

1. It is possible to materially improve the soundness of ferrous die castings by appropriate thermal design of the dies.
2. Rheocasting processes are possible for steels, but their potential advantages over present ferrous die casting techniques need further study.
3. Mold life is a key problem to any ferrous machine casting process.

II. PERMANENT MOLD CASTINGS - GREY IRON TEST SHAPE

A mold test shape was designed as shown in Fig. 1. It has two thick sections connected by a thin web. The shape was chosen to define problems encountered in feeding thick and thin sections and problems encountered with changing cross section.

The initial choice of mold material was a grey cast iron. Grey iron was chosen for ease in fabrication. For a true commercial process where long life would be required, mechanical and physical properties might dictate other choices.[1-2] but mold material was not central to this investigation at that time. A pattern was made in wood of the mold shape and grey iron cast into sand molds made with this pattern. The grey iron alloy chosen is listed in Table I. It had 0.40% Cr added to stabilize the pearlite, since the permanent mold would see temperatures where the pearlite would graphitize, leading to dimensional changes. The grey iron castings tended to have a heavy chill of white iron on the surface, and cracks due to hot tearing. It was felt these problems were due to the Cr content, and the alloy was changed to one containing 0.20% Cr. This composition is also listed in Table I. Mold castings were satisfactorily made from this alloy. The microstructure of this second alloy is shown in Fig. 2.

TABLE I

	C	Si	Mn	Cr	Fe
Initial Alloy	3.35	2.35	0.6	0.4	bal.
Final Alloy	3.54	2.35	0.6	0.2	bal.

Two molds were cast in this second alloy. After light machining of the mating surfaces and smoothing of the mold inside surfaces, they were stress-relief annealed at 1100°F.

The permanent mold had a pouring basin atop it. The pouring basin was essentially a "vee"-shaped trough with the opening at the bottom a thin slit. It was felt that surface finish would be best if metal fell through the gate as a sheet and rolled up the sides of the mold, rather than in a feeding arrangement with more open gates which would tend to have unsteady streams of metal. In such latter cases, metal hitting the wall would immediately freeze, leaving a rough surface. The pouring basin was made of a high-fired alumina ceramic. The pouring basin on a mold is shown in Fig. 3.

It was initially felt that the pouring basin, even with its narrow opening would feed the solidification shrinkage due to the high thermal conductivity of the mold compared with that of the ceramic basin. Since the upper surface of molten metal would be in contact with the lower surface of the pouring basin, the heat from the pouring basin would direct the solidification front in an upward manner.

The surface of the mold was coated with a commercial Zircon mold wash applied as a slurry. The slurry was air-dried on the mold at 400°F.

Master heats weighing 75 lbs. were made up of IN-738, TRW VI A, Mar M 302, Mar M 509 and 304 Stainless Steel. The heats were vacuum melted in 25 lb. ingots. The compositions are listed in Table II.

The intent of the experiments on casting was to duplicate in an individual casting one cycle of an automated process. Mold temperature and metal superheat were varied on individual pours.

Castings were made in an induction furnace under an argon atmosphere. The mold was preheated with nichrome wound heating plates. The mold sat on a graphite block. Melt, mold and casting temperatures were monitored with thermocouples. Normal casting procedure was to heat the mold to the desired temperature; melt and freeze the alloy in its crucible, recording the liquidus

TABLE II

	Ni	Co	Fe	Cr	Al	Ti	Ta	Cb	W	Mo	Hf	Zr	B	C	Re	Mn	Si
IN-738	bal.	8.5	-	16.0	3.4	3.4	1.75	.9	2.6	1.75	-	.10	.01	.17	-	-	-
TRW VI A	bal.	7.5	-	6.0	5.4	1.0	9.0	.5	5.8	2.0	.43	.13	.02	.13	.5	-	-
Mar M 302	-	bal.	-	21.5	-	.75	9.0	-	10.0	-	-	.15	.005	.85	-	-	-
Mar M 509	10	bal.	1.0	21.5	-	.2	3.5	-	7.0	-	-	.50	.01	.60	-	-	-
304 SS	8	-	bal.	18.0	-	-	-	-	-	-	-	-	-	-	-	1	.5

arrest; reheat the alloy to the desired superheat; and pour the casting.

Castings of IN-738 were made varying superheat from 50 to 100°C and mold temperatures of 200°C and 400°C. Findings indicated that major departures were required from all-metal mold practice.

First, in all cases, the casting was wedged severely in the mold. The castings had to be removed with a chisel. The reasons for this lie in the thermal response of the mold and in differences in thermal expansion.

The thermal response of the mold is shown in Fig. 4. Thermocouples monitored temperature 1/4" in from the mold face in the thick section of the casting, and a thermocouple was inserted into the casting. As can be seen, the casting is solid within 50 seconds after pouring, and is rapidly cooling. However, the mold temperature rises for about 250 seconds. Then the casting is shrinking while the mold is expanding. This will lead to a mechanical interaction locking the casting into the mold. Then, even after both mold and casting are cooling, grey iron has a lower thermal expansion coefficient than the casting, further locking the casting into the mold.

Second, due also to the mechanical interaction between mold and casting, all castings had cracks in the thin web section of the casting. The extent of these hot tears can be seen in Fig. 5, a microphotograph of the web section of a casting.

Third, it was felt that the pouring basin would tend to minimize shrinkage or at least move it into the upper section of the casting. This turned out not to be so, as can be seen in Fig. 6. There is a deep shrinkage pipe which extends down into the lower half of the casting.

This gross porosity contrasts strikingly with the absence of severe interdendritic microporosity in IN-738. This can be seen in Figs. 7 and 8. These areas are away from the center shrink.

The absence of large amounts of microporosity indicates much about the mode of solidification. The alloy is solidifying not only rapidly, but under a sufficiently high temperature gradient that the physical distance between the dendrite tip at the solidifying point and the last solid to freeze is very short, allowing free flow of liquid back to this latter area. The large shrinkage pipe occurs when the casting simply runs out of liquid.

Another aspect of the microstructure of these castings is the relative absence of segregate phases associated with IN-738 grown at 1/4"/hour in a Bridgeman furnace. There are large pools of a eutectic as well as large blocky MC carbides. Large section size castings, in which these microstructural features are frequently found, tend to have poorer mechanical properties compared with thinner sections.[3]

There were two problems to solve as a result of the initial casting results. The first problem is the mechanical interaction between mold and casting. The second is the need to feed adequately the casting.

To reduce the thermal expansion mismatch requires choosing a new mold material. Even with a new material, however, the mold expanding while the casting is contracting will lead to hot cracking or hot tearing.

For other casting geometries, where the casting is not going to be locked at both ends, any mold material which withstands thermal shock might suffice. However, for this severe a shape, it is impossible to remove mechanical constraints. A new mold concept was defined, where parts of the mold would yield under stress rather than the casting. Using disposable pieces for these sections, a mechanical casting process can be pictured where after a casting is ejected, new crushable inserts automatically placed in the mold, and the mold closed for a new casting.

For adequate feeding of the casting, gating systems as used in die casting are clearly insufficient. Gates in die casting are always thin and small, designed from a standpoint of minimum wasted metal and ease in removal. To get a molten supply of metal to feed the casting, a small ceramic riser is necessary. This pool of metal, cooling less rapidly than the casting in the metal mold, would feed. The riser also could be a disposable insert placed in the gate section of the casting. In a machine casting process, it could be ejected with the casting and a new one automatically placed on the gate.

To test these concepts, new cast iron molds were made, of the same alloy as the original molds. Fig. 10 shows such a mold. The center section where the mechanical interaction occurred, is left open, and in it ceramic inserts are placed as shown in Fig. 11. The inserts were made from a high alumina CO_2 setting sand. The holes in the inserts were designed to aid in crushability. Only the corners of the mold web need have been made of ceramic, but for experimental ease, the entire section was made of a one-piece ceramic.

The riser used is shown in Fig. 12. It also was made from a high alumina CO_2-sand. The riser need not have been the shape of the casting. It would well have been two ceramic tubes over the two thick sections of the casting; but for experimental convenience, it was left in the casting shape.

The total assembly of mold, riser, and pouring basin is shown in Fig. 13. The mold and riser would have heaters placed around them during casting. Castings of TRW VI A, Mar M 302, IN-738 and 304 Stainless Steel have been made in this modified mold.

The casting arrangement greatly improved casting soundness. The gross shrinkage was confined to the riser area. The crushable inserts prevented hot tearing and cracking in the web section. The increase in soundness can be seen in Figs. 14 and 15. These are X-ray photographs of two castings. In Fig. 14 is

Mar M 302 poured at 1430°C (100°C superheat) and mold temperature 400°C. The only observable defect is in the region of changing cross section on the upper left. This is a small shrinkage pipe due to faulty pouring. The metal stream poured against this part of the mold and created a hot spot.

Fig. 15 is an IN-738 casting poured at 1430°C (100°C superheat). The only observable defects were in the thick section exposure shown. These turned out to be surface pits rather than internal shrinkage voids.

Aside from eliminating cracks, the inserts had other effects, - notably, to slow down solidification in the thin section. Fig. 16 shows the thermocouple recordings of the Mar M 302 casting shown in Fig. 14. The thermocouples are located in the mold, one touching the back of the insert and another in the end, 1/4 inch in from the mold face. A third thermocouple extends into the center of the casting in the thick section. As Fig. 16 shows, the insert temperature rises much slower than the outer mold. Heat is removed much more slowly.

The microstructure of the castings also reflect this difference in heat extraction. Figs. 17 and 18 are photomicrographs of Mar M 302 cast at 1430°C and initial mold temperature of 400°C. Fig. 17 is of the thick section, and Fig. 18 is of the thin section. Both areas photographed are near the center of their respective section. As can be seen, the ceramic inserts have now made the thin section freeze slower than the thick. Qualitatively, both microstructures are the same. Cobalt dendrites and an interdendritic cobalt-MC carbide eutectic make up the bulk of the microstructure with the final liquid to freeze being an M_6C-$M_{23}C_6$ eutectic which appears as dark unresolved pools in the photomicrographs. The thick section has a much finer dendritic structure indicative of its higher growth rate than the thin section. Both sections differ from investment cast material as to amount of Co dendrites. In investment cast Mar M 302, there are few Co-dendrites. The investment cast microstructure has a higher amount of Co-MC and M_6C-$M_{23}C_6$ eutectic.[4] The larger amount of Co-dendrites in the

permanent mold cast microstructure is most likely due to the eutectic carbides requiring a higher kinetic under cooling than Co, resulting in a shift in observed eutectic composition at the high growth rates occurring in a chill casting.[5]

TRW VI A shows the same general effects as Mar M 302. Fig. 19 is a thick section and Fig. 20 a thin section of a permanent mold casting poured at 1430°C and 400°C mold temperature. The microstructure in both sections is Ni-base dendrites with a fine dispersion of MC carbides and pools of a γ-γ' segregate eutectic. The sections have been etched to show the γ' precipitate in the Ni-base dendrites. As in Mar M 302, the structure is much finer in the thick section of the casting than in the thin, indicating that the ceramic insert is having considerable thermal effect.

TRW VI A also has a certain amount of microporosity associated with the γ-γ' eutectic. This differs from the behavior of Mar M 302, where no porosity was found in the last area to freeze, - the M_6C-$M_{23}C_6$ eutectic. This porosity is shown in Fig. 21. TRW VI A has a high B and Zr content. Both B and Zr have low distribution coefficients with Ni, - the ratio of concentration in the solid to concentration in the liquid, C_s/C_L, is very low. It is likely that in the case of TRW VI A, that there is a liquid to freeze left after the γ-γ' eutectic is solidified. These small volumes of liquid are no longer interconnected and are then not fed.

IN-738 and 304 Stainless Steel have also been solidified in modified permanent molds. Their general behavior is similar to the above discussed castings. Dendritic structure is coarser in the thin section than in the thick. In the case of IN-738, there are small areas of scattered porosity, not in the quantity seen in TRW VI A and not large enough to be observed by X-ray transmission photographs. It is porosity typical of large section size investment castings of the same alloy.

304 Stainless Steel has been cast without the ceramic inserts but with the ceramic riser. This casting made shows a slight amount of porosity near the center of the casting, but no inter-dendritic porosity.

III. PERMANENT MOLD CASTINGS - BLADE SHAPE

To further evaluate the ability of ceramic inserts to feed castings made in permanent molds, blocks of ZRBSC-M(R), a Norton Co. ceramic, were machined to cast a blade shape as shown in Fig. 22.

ZRBSC(R) is an experimental ZrB_2-SiC-Graphite material manufactured by Norton and proposed for uses in metal gating systems, chills in permanent molds, and die casting molds. This material was chosen for the mold to evaluate it for use as chilling inserts or complete molds for ferrous casting.

An alumina tube was used as the gate and riser in the blade mold as shown in Fig. 23. A larger alumina tube was slid over the insert tube and glued to it to prevent the smaller tube from sliding into the mold. The mold halves were clamped together on their ends by steel clips.

Two castings were made of Mar M 302. Pouring temperatures were 1430°C and mold temperatures were 550°C and 700°C. Temperatures of the mold was monitored by thermocouples on the back of the mold in the center of the thin section and at the center of the root. Maximum temperatures reached by the mold were 680°C and 820°C for the low and high initial mold temperatures. As in the case of the cast iron molds, this temperature was reached about 200 seconds after pouring.

On the first casting, the mold developed large cracks in the root section. The cracking occurred while the metal was still molten; the cracks left impressions in the casting. Fig. 22 shows the mold after the first casting. It is likely that the mold cracked as the first metal entered the root section. The thin section of the mold did not crack at all. Presumably, the amount of metal being less, and the metal temperature being lower, reduced the thermal shock in this region.

The second Mar M 302 casting was made after clamping the mold together. No new cracks opened up. The mold has been repaired with a mixture of potassium silicate and powdered graphite.

The casting is shown in Fig. 24. The alumina insert tube has been removed. The surface of the casting shows flow lines, which indicate the need for a mold coating to slow down the initial rate of freezing. Fig. 25 shows two cross sections through the casting. Referring to Fig. 24, after removing the riser, a vertical slice was made through the root section, then a horizontal slice was made through the blade section. As can be seen, the structure has no gross porosity associated with it.

The microstructure is shown in Fig. 26. It is the same type as seen in Figs. 17 and 18, but finer, indicating a higher rate of solidification. No porosity was found in the specimen.

The soundness in the blade casting indicates that a simple insert system works for this shape as well as the cast iron mold shape, at least for Mar M 302. No other castings were made in ZRBSC, since it is felt that the condition of the mold could effect results.

The blade shaped mold was fabricated in an austenetic grey iron. Castings of all alloys were made in this shape. It was found that a 3" riser insert was sufficient to make sound castings in MarM302, MarM509, and 304 stainless steel. A pouring temperature was not critical, but between 100-150°C superheat gave a good surface finish.

The blade-shaped mold was fabricated in an austenitic grey iron. The composition of this alloy was Fe-20%Ni-5%Cr-2.52%C-2.67%Si. Further castings of all alloys were made in this mold.

It was found that a 3" ceramic insert riser was sufficient to give sound castings in Mar M 302, Mar M509, and 304 stainless steel. Castings of IN-738 and TRW Vla showed small, isolated amounts of interdendritic porosity which could not be fed by the riser. The porosity in IN-738 was not severe, but in TRW Vla was similar to that discussed in Section II.

IV. SURFACE FINISH

The surface of the castings made in the cast iron molds and in the ZRBSC molds contained numerous folds and flow marks. In addition, the inserts and riser in the cast iron molds caused the appearance of small bubbles near the surface of the casting. These bubbles are gas filled and due to the breakdown of the binder in the ceramic as the hot metal contacts it.

Inserts were constructed out of high-fired zircon. The riser was left in CO_2 setting alumina because the pouring basin is such that no molten metal reaches the riser until the mold is filled, and it is felt that the gas bubbles that occur on the casting surface are due to the immediately adjacent ceramic. Since the metal freezes so quickly, gas bubbles would not be able to move into the casting. Also, since the riser is at the top, even if gas bubbles did form and get into the metal in the riser, they would float up, away from the casting.

The surface irregularities pointed out the need for the liquid metal to be able to form against the wall of the mold before it freezes. The zircon wash used was not enough of an insulator to prevent the immediate freezing of a skin of metal.

Both an insert mold and an all-metal mold were plasma sprayed with ZrO_2. The thickness of the coating was 5-10 mils. An IN-738 casting made in the insert mold at 400°C initial mold temperature, poured at 1470°C is shown in Fig. 27. A 304 Stainless casting was made in the all-metal mold at 600°C mold temperature and 1550°C pouring temperature. It is shown in Fig. 28. In both cases, the surface was markedly improved, with no serious flaws. Thermocouple readings during solidification show no difference between the plasma sprayed coatings and the zircon wash coatings.

The amount of time initial solidification need be delayed to effect a good surface is probably much less than 1 second, since all that is required is for the liquid to be able to smooth out any ripples before it freezes. The thin layer of ZrO_2 provides this.

The durability of a plasma sprayed coating is not that great. In the insert mold, it has lasted through 5 castings without spalling off, but it shows areas of cracks. However, the plasma coating has shown what thermal properties are needed for good surface finish.

V. RHEOCASTING

Rheocasting[6] is the technique whereby liquid-solid slurries of alloys are cast into molds, rather than pouring a liquid. The technique was developed in low-melting alloys and has been extended to copper base alloys (m.p.<1000°C).

The technique of slurry preparation is to fully melt and then cool the alloy to a temperature where it is a liquid, solid "mush" while stirring. The slurry can be directly cast into a mold, or cast into slugs which are later reheated for casting.

The slurry is cast at a lower temperature into the mold than a normal, all-liquid casting and thus might provide a reduction in thermal shock to the mold. It is this potentially improved mold life that would justify the added manufacturing steps in the ferrous die casting process that rheocasting would require.

A rheocasting machine was designed and constructed as shown in Figure 29. The machine used a variable speed d.c. motor run through a gear train. An austenitic shaft drove a paddle which could be raised and lowered into an induction heated melt. The apparatus was attached to a vacuum induction furnace capable of melting 20 lbs. of metal.

A key problem with rheocasting is obtaining a paddle material which can withstand the mechanical forces, thermal shock, and reaction with the melt. Since these are not severe requirements with rheocasting aluminum alloys, copper alloys, or cast irons, it was felt that nothing would be learned from a research program which studied rheocasting in aluminum, copper, or cast irons, as the material problems for steel would not be solved. 304 stainless steel was chosen as the alloy to rheocast, with one rheocasting made of IN738.

Three paddle materials were evaluated - low-density alumina, high-density alumina, and zirconia-coated molybdenum. All alumina paddles failed due to thermal shock, while the molybdenum paddles performed very well, with no failures.

The mold used for rheocasting was a blade-shaped mold similar to that of Figure 23, only made in grey iron. The composition of the mold was Fe-20%Ni-5%Cr-2.52%C-2.67%Si. The mold is shown in Fig. 30. To measure the thermal response of the mold during casting, thermocouples were welded into the mold as shown in Figures 31 and 32. The thermocouples on the face and edge positions extend up to the mold cavity where they are welded to the mold surface.

The method of rheocasting is to melt the alloy, cool it and pick up its solidification temperature on a thermocouple on the crucible. The alloy is then remelted, the paddle lowered, and stirring begun. The temperature is slowly lowered until the paddle stalls, then the alloy is remelted. The temperature is lowered to 10°C above the stall temperature with the paddle stirring; the alloy is stirred for 5 minutes, then the casting is poured. The mold temperature is monitored on a multipen X-t recorder.

Typical results with the use of an alumina paddle are shown in Figure 33. The paddle cracked, failed to stir the slurry sufficiently, and the casting did not fill. Based on experience with both low- and high-density alumina, ceramic paddles were ruled out. Carbon bearing paddles (such as plumbago) were also ruled out due to reaction with the melt.

Molybdenum paddles, plasma-sprayed with ZrO_2, worked very well. The paddles did not crack under thermal shock, and the coating did not spall off during immersion in the melt. Several

successful paddles are shown in Figs. 34-36. In Fig. 34, a multiple-slotted paddle is shown after use. The metal adhering to the paddle is locked on due to the slots, but has not reacted with the paddle. Similarly, in Fig. 35, a paddle with two holes was used. No wetting of metal, but metal mechanically locked on. Fig. 36 shows the most successful paddle. It is a two-bladed design. Metal is shown adhering, but it can be peeled off as it is not mechanically locked and did not wet the paddle.

Two rheocastings made with the plasma-sprayed molybdenum paddles can be seen in Fig. 37. The surface finish is not good, but the casting filled, as compared with Fig. 33. The better stirring with the molybdenum paddles kept the solid particle size small, and the slurry had better flow characteristics. The surface finish is quite poor, however, when compared with an all-liquid pour casting of the same alloy, 304 stainless, poured at 100°C superheat (1550°C), shown in Figure 38.

Microstructures of 304 stainless and IN738 differ markedly between conventionally cast and rheocast. Figure 39 shows the difference in grain size between a rheocast and conventional chill cast IN738. The sections shown are through the thick area of a blade casting. The rheocast grains are very fine and show no directionality, while the conventional cast grains are columnar from the casting surface. Figure 40 shows the center of a blade casting of 304 stainless rheocast and conventional cast, and Figure 41 shows the same areas at higher magnifications. As can be seen, the conventional casting has a dendritic pattern, which is masked somewhat by the dark ferrite which transformed in the solid. The rheocast structure is that of islands of austenite with transformed ferrite surrounded by pure austenite. There is no evidence of a directional structure, and it can be presumed that each island was a separate solidification center.

Thermal data from the mold response to casting is shown in Table III and in Figure 42. There appears to be little difference in mold temperature rise among rheocasting, conventional casting at 1500°C and conventional casting at 1550°C. Only when the pouring temperature is 1600°C does there appear to be a significant difference in mold face temperature rise. However, as seen in Figure 42, the mold cools slightly faster with a rheocasting. This latter effect is due to there being less heat in the rheocasting as some latent heat of fusion was removed in the crucible.

To further measure thermally induced stresses, a thermocouple was placed .100 inch in from the face of the mold, opposite the "face" thermocouple. The "face" thermocouple and this latter thermocouple were connected together to measure ΔT - t curves, to give a measure of temperature gradient vs. time in the mold. Castings were made of 4340 steel, 304 stainless steel, and IN738, both rheocast and at 100°C superheat. No significant differences were found in either time rate of rise of ΔT or in maximum ΔT between the two cases.

It should be noted that the thermocouple measures temperatures over 10 mils (the size of the bead), and at the casting-mold interface, the temperatures are different. But the thermal fatigue crack growth is due to the ΔT; and since the mold surface can be presumed to have flaws which can act as fatigue cracks, the life of the mold is determined by crack growth rate, not time to initiation of the crack.

In the development of a ferrous die casting process,[1] 304 stainless steel was cast from a temperature of 1500-1600°C. Our initial data suggests that rheocasting treats a mold just as severely as such a casting process.

Further, in our experiments with casting at 1500-1600°C, the metal was poured directly into a mold. In a die-casting process, the metal is poured into a shot sleeve and must pass through a gate-and-runner system to arrive at the mold. In both the shot sleeve and the gate-and-runner system, the

metal is transferring heat. In the die-casting system, the initial metal pour is 1500-1600°C, but the metal arriving at the mold is appreciably cooler. Some of the microstructures shown for 304 stainless suggest that in a die-casting process, the metal was already part solid as it reached the mold cavity, since the microstructures are more similar to the rheocast microstructures of this work, as discussed in Section VIII.

If the normal practice of ferrous die casting is such that the metal arrives as a liquid-solid slurry due to heat losses in the gate-and-runner systems, there is no further advantage to rheocasting, since the metal will arrive at the same temperature by either technique. Mold lives by either technique will be comparable.

TABLE III

304 STAINLESS

Type	T.C. Position	Pour Temp. (°C)	Max. $\frac{dT}{dT}$ (°C/sec)	Max. Temp. (°C)
Rheocast	Face	1410	∿320	780
Conventional	Face	1540	∿395	740
Rheocast	Edge	1420	∿700	920
Conventional	Edge	1500	∿700	1010
Conventional	Edge	1550	∿800	1010
Conventional	Edge	1600	∿1300	1240
	IN 738			
Rheocast	Face	∿1330	280	600
Conventional	Face	1420	280	640
	4340 Steel			
Rheocast	Face	∿1480	320	640
Conventional	Face	1604	330	650

VI. ALLOY MODIFICATIONS

To improve the soundness of TRW VI A and IN-738, both the B and Zr content of these alloys was reduced. TRW VI A normally has .02 B and .13 Zr; IN-738 - .02B and .10 Zr. Contents were reduced to .005B and .05 Zr for both alloys. Both alloys were cast into the cast iron insert molds at 400°C mold temperature and 100°C superheat above their respective liquidi.

Both microstructures were markedly changed. IN-738 lost the last vestiges of the segregate eutectic in it. TRW VI A had a drastic alteration of the γ-γ' segregate eutectic. This is shown in Fig. 43. What is left of the eutectic has taken on the appearance of the "swirly γ'" obtained in Hf-modified superalloys.[7] Microporosity appears to have decreased.

Tensile bars were cut from both castings and tested in stress rupture. The uniformly poor results were due either to residual porosity or the change in alloy chemistry was detrimental to properties, irrespective of casting soundness. To test this latter assumption, the modified composition of TRW VI A was cast into tensile bars in an investment mold. The bars show no signs of porosity, yet the properties were similar to the alloy cast in the cast iron chill mold.

It is safe to assume that the reduction in porosity was more than offset by the reduction in mechanical properties due to the alloy changes. Work in this area has stopped.

Mechanical properties are reported in the next section.

VII. MECHANICAL TEST RESULTS

Mechanical test specimens have been electrical discharge machined from both the castings made in the cast iron mold and from the blade mold. Tests made have been stress-rupture and tensile.

The results vary with the alloy, and are in agreement with the general observation of microstructure and soundness. TRW VI A, Mar M 302, Mar M 509, and 304, and 4340 steel have been tested as-cast, IN-738 is tested after heat-treating at 2050°F, 4 hours, and then 1500°F, 24 hours.[8] Test conditions were chosen to give lives of 100 hours or less. Test results are summarized in Tables V and VI and in Larson-Miller plots shown in Figs. 44-52. The solid lines in Figs. 44-52 were constructed from published data.[9]

The data for TRW VIA is plotted in Fig. 44. The data from this study all lie below the average properties of TRW VIA. Examination of bars after rupture show large cracks opening up from the γ-γ' eutectic, probably associated with microporosity. This eutectic may be a source of porosity in investment cast TRW VIA as there is considerable scatter in data obtained in cast-to-size tensile bars.[10,11]

The properties for IN738 are shown in Fig. 45. All data lies uniformly below the average curve for cast-to-size bars. Data for large size castings shows a reduction in properties[3] compared to cast bars,[8] and our data lies on the low end of the scatter band for large castings.

Mar M 302 and Mar M 509 both solidifed with low levels of porosity. This is reflected in the stress rupture behavior and is shown in Fig. 46 and Fig. 47. In both alloys, the properties of the castings are equivalent to cast-to-size rupture bars.

Conventional and rheocast 304 stainless and 4340 steels were tested in stress rupture for 304 stainless and in tensile tests for both alloys. Stress rupture properties are shown in Fig. 48 and Table V. Tensile properties are shown in Figs. 49 and 50 and Table VI. As can be seen, the properties are equivalent to standard wrought product. The properties of conventionally cast and rheocast 304 are equivalent except for tensile ductility shown in Fig. 50, where the rheocast properties are slightly lower.

The properties of the modified TRW VIA and modified IN738 are shown in Fig. 50 and Fig. 52. As can be seen, the modification made no improvement on stress rupture properties in spite of reducing the porosity. Cast-to-size tensile bars were made of modified TRW VIa, and its stress rupture properties were equivalent to the permanent mold cast properties indicating that the modification degraded the mechanical properties. In Fig. 52, the average value for the permanent mold casting is plotted along with the properties of investment-cast, non-modified IN738. The properties of the modified permanent-mold castings are equivalent to those of the normal permanent-mold castings.

VIII. FERROUS DIE CASTING

An aluminum die casting machine was modified for die casting ferrous alloys. The intent of this aspect of the work was to study the effects of casting temperature on the mold thermal response and to evaluate changes in metal feeding as a function of section size and use of ceramic inserts.

For ease in fabrication and since long die life was not required, the die insert was made from austenitic grey iron. The mold design is shown in Fig. 53 and Fig. 54. Fig. 53 is a drawing to size and scale of the die insert. The metal enters from the shot sleeve at "S", travels up the runner system, and back into the mold cavities. Two Pt-Pt-10% Rh thermocouples

were welded onto the die insert face at the positions marked by the open squares. Alumina inserts were placed in the die at the positions marked by a "C" in Fig. 53, to aid in improving casting soundness. At the end of each leg of the casting, there was an over flow and vent marked in Fig. 53 by "O". Ejector pins were located behind the ceramic inserts and one located at the base of the gate, just opposite the shot sleeve. An advantage of the ceramic inserts was also to prevent metal from "finning" down the ejector pins. The die was heated from calrod units placed in holes drilled through the die set. To protect the shot sleeve and plunger, a graphite wafer was inserted against the plunger tip, and a Fiberfrax(R) cloth was placed on the bottom of the shot sleeve. After casting, the Fiberfrax(R) cloth was matted in the biscuit, and the wafer was on the end of the biscuit where it could be removed and used again, if desired.

The mode of operation was to put inserts into their respective cavities, close the die, place the Fiberfrax(R) cloth on the bottom of the shot sleeve, and insert a graphite wafer against the shot ram tip. Then, molten metal is poured into a preheated ladle and transferred to the shot sleeve. Upon pouring the metal, the ram is actuated and the casting made.

To test the mechanical operation of the die casting machine, castings of Al-13%Si were made. The machine worked excellently and the castings made had both good surface finish and reasonable soundness. The die casting machine is shown in Fig. 55, and representative aluminum die castings in Fig. 56-58.

Die castings were then made from 304 stainless steel. The die temperature was set at 200°C. Plunger speed used was 8 inches/sec. Metal temperatures on casting were varied from 1484°C to 1555°C (34°C to 105°C superheat above liquidus).

The die face was coated with a zircon wash prior to initial use. After several shots, the die was sprayed with colloidal graphite. During monitoring of temperatures on the die face, it was found that the thermal response of the mold in casting was a strong function of this coating with a graphite film.

The temperature rise on the mold face during casting was essentially instantaneous. The maximum temperature reached on the surface did not vary directly with superheat, but with whether the mold had been previously washed with graphite. This is shown in Table IV. After castings 7113, 7115, and 7116, the mold was sprayed with graphite. The casting made immediately thereafter caused a lower maximum observed temperature for the same or a higher superheat.

TABLE IV

Casting	Casting Temperature	Maximum Temperature
7112	1512°C	560
7113	1515°C	570
7114	1535°C	545
7115	1552°C	610
7116	1555°C	575
7117	1484°C	590

Within the temperature range studied, superheat had little effect on surface finish. Fig. 59 shows casting 7117, the lowest superheat and Fig. 60 shows casting 7115, the highest superheat.

One casting was made with copper sleeves replacing the ceramic inserts, to duplicate more conventional practice where no provision is made for feeding the casting. This casting, 7116, is shown in Fig. 61.

X-ray photographs of the die castings were made to evaluate soundness. A composite of the X-ray photographs is shown in Fig. 62. The extensive porosity in the riser areas indicates that the ceramic inserts did feed the casting. From Fig. 62, it appears that the most sound castings were made at the lowest and highest superheats. Presumably, at the lowest superheats, the feeding was more difficult, but there was less liquid shrink to feed, while at the highest superheats, the ceramic riser got sufficiently hot to stay open long enough to feed the entire bar. At intermediate superheats, the riser froze off before it could completely feed the bar.

Typical microstructure of the castings is shown in Fig. 63. It is very similar to that of rheocast 304 shown in Figs. 40 and 41. This microstructure is that of all die castings - from the lowest to the highest superheat. It can be presumed that sufficient heat was lost in the gate-and-runner system that the metal was below its liquidus temperature when it arrived at the mold cavity, essentially at the same temperature that a rheo die casting would have to be, in order to fill the mold.

IX. DISCUSSION

The work to date on obtaining integrity in permanent mold rapidly solidified castings and die castings has shown three things - there is a need for thermal conditions to allow adequate feeding of solidification shrinkage, certain alloy types respond better to a rapid solidification process, the quality of the surface finish strongly depends on mold coating.

In a normal die casting process, where the in-gates are narrow, the thin gate area freezes soon after solidification starts. Then the metal in the die cavity has no source from which to feed its shrinkage. To assure adequate feeding with an all-metal mold and gate system, the gate would have to be quite large. For the gate to simply remain molten during the time the casting is solidifying, the gate would have to be as large as the thickest section of the casting. However, even a molten gate does not assure adequate feeding if, for example, the thickest section of the casting is separated from the gate by a thinner casting section. In order to assure feeding in such a case, the gate must also supply heat to the thin casting section so that the solidification front moves toward the gates. The size of a gate to do this in an all-metal mold could easily become quite large, increasing not only scrap losses, but also mold and finishing costs. The use of a ceramic insert in a gating section can reduce this size needed. The insert can hold sufficient heat to set up a desired thermal gradient in the casting.

In an automated machine casting process, such an insert could be automatically placed in a mold, a casting made, and the insert ejected with the casting. Inserts need only be off-the-shelve ceramic tubes which fit the gate. The ceramic need not be disposable. If the ceramic is such that it can take thermal shock and the wear of the rapidly flowing metal, it could be a permanent part of the mold.

Alloy type appears to be quite important in obtaining sound structure. Mar M 302 has shown low levels of porosity and good properties in permanent mold castings, while both TRW VI A and IN-738 have certain amounts of microporosity and degraded properties. The microstructure of TRW VI A indicates that the last liquid to freeze, near the γ-γ' eutectic, is isolated from the main pool of liquid. In such a case, there is no feeding and a small pore is left. In Mar M 302, the Co dendrites are a smaller fraction of the microstructure than are the Ni dendrites in TRW VI A or IN-738. The interdendritic liquid which freezes in Mar M 302 has much easier channels to feed.

This should be a general case, that alloys with long freezing ranges, with a gradual decrease in liquid with temperature tend to have a more severe microporosity problem than those which freeze over a more narrow temperature range. The high freezing rate and high gradient reduce the physical length of the liquid to solid zone in the casting. This would tend to help most materials with very short freezing ranges.

Surface finish has been greatly improved by use of a more insulative mold coating. To avoid entrainment of gas, mold filling rates have been less than in a die casting process. This slower filling rate results in a tendency for the metal to freeze irregularly on the surface. A coating which allows the metal to form against the mold can reduce this. What is required in the coating is that its surface heat rapidly and hold that heat for a short period of time, keeping the metal molten. In addition, the coating must not release gases to get into the melt as the rapid rate of freezing is such that the bubbles can't rise out of the casting, but are trapped near the surface.

Rheocasting process development has shown promising paddle materials, and demonstrated the process for steels and superalloys. Up to this point, copper-base alloys and grey irons were the maximum melting point materials rheocast. The rheocast stainless steel had a strikingly different microstructure compared with conventionally cast 304. Properties of the rheocast 304 stainless and 4340 steels were equivalent to the conventionally cast.

Mathematical analysis[2] predicts a difference in temperature rise rates on a mold face between casting a metal slurry and casting an all-liquid melt, due to temperature differences of the cast metal. However, this difference in thermal response between casting processes is most severe only in the outer few mils of the mold, where the surface is already presumed to have flaws and the mode of mold failure is from crack growth. Hence, the prediction is that while on the mold surface there is a difference in thermal response to the casting processes, there is no difference a few mils into the mold. There should be no difference in thermal fatigue life.

These predictions were verified by measuring the thermal response of a mold during rheocasting and conventionally casting steels. Thermocouples were welded at various parts of the mold, including on the mold face. No differences were seen between rheocasting and conventional casting at superheats typical of ferrous die casting. The width of the thermocouple bead was such that temperatures were measured over 10 mils rather than just at the surface; but, as mentioned above, any differences in temperature rise right at the mold surface are probably inconsequential to life of the mold in thermal fatigue.

The ferrous die casting made during this work all had microstructures typical of Fig. 63. This microstructure is similar to that in Fig. 41a, a rheocasting in a permanent mold. It appears that, in the die casting process used, while the metal enters the shot sleeve in the liquid state, it loses

sufficient heat in the shot sleeve and runner system that it is below the liquidus temperature when it reaches the mold cavity. A significant contribution to the heat removed from a casting is the latent heat of fusion; the rheocasting may reduce the heat removal requirements on the mold by its having a higher fraction solid on arrival at the mold. This factor could give improved mold life for rheocastings compared with conventional ferrous die castings.

It was not possible to estimate the fraction solid of the metal in the die, and compare this with the fraction solid of a hypothetical rheocasting process; but since the freezing range of 304 stainless is about 50°C, the temperature of the metal arriving in the mold cavity in the die casting process would have to be close to that which would occur in rheocasting.

There are two chief implications with respect to the application of rheocasting to a ferrous machine casting process. The first is that since considerable heat can be lost in the shot sleeve and runner system, the rheocast slurry could freeze off before filling the mold unless the shot sleeve and runner is either eliminated or insulated.

The second implication is due to the similarity in metal temperatures in the mold cavity between conventional ferrous die casting and that which rheocasting would have, and due to the inability to measure large differences in mold face temperature rise between rheocasting and all liquid casting in chill molds. There is therefore a strong need to more carefully evaluate the potential advantages of rheocasting as pertains to mold life in particular. This comparison should take into account the fact that in the present machine casting process, the metal can arrive at temperatures comparable to rheocasting. Since life testing molds would involve 50,000 - 100,000 castings, emphasis in the near term should be on thermo-mechanical modeling of molds during casting.

REFERENCES

(1) D.J.McMillin, "A High Temperature Alloy Die Casting Process," Technical Report AFML-TR-69-223 (1969).

(2) S.J.Noesen and H.A.Williams, "The Thermal Fatigue of Die Casting Dies," Paper 801, Transactions, Fourth National Die Casting Congress, Society of Die Casting Engineers (1966).

(3) G.E.Wasielewski and N.R.Lindblad, Paper D, Proceedings Second International Conference Superalloys--Processing, Battelle Report MCIC 72-10 (1972).

(4) C.P.Sullivan, M.J.Donachie, F.R.Morral, "Cobalt Base Superalloys-1970," Centre d'Information du Cobalt, Bruxelles (1970).

(5) J.D.Hunt and K.A.Jackson, Transactions TMS-AIME, v. 239, p. 864 (1967).

(6) C.G.Bieber and J.R.Mihalisin, Paper 17.1, Proceedings Second International Conference on the Strength of Metals and Alloys, ASM, p. 1031 (1970).

(7) W.F.Simmons, "Compilation of Chemical Compositions and Rupture Strengths of Superalloys," ASTM Data Series Publication No. DS 9E (1970).

(8) H.E.Collins, "Development of High Temperature Nickel-Base Alloys for Jet Engine Turbine Applications," Report TRW ER-7042, Contract NAS 3-7267 (1966).

(9) H.E.Collins, "Development of High Temperature Nickel-Base Alloys for Jet Engine Turbine Bucket Applications," Report NASA CR-54507 (TRW ER-7162), Contract NAS 3-7267 (1967).

(10) P.S.Kotval, J.D.Venables, and R.W.Calder, Met. Trans., v. 3, p. 453 (1972).

(11) R.Mehrabian and M.C.Flemings, Transactions AFS, v. 80, p. 173 (1972).

TABLE V

	Mold	σ(ksi)	T(°F)	Life (hours)	P_{20}
TRW VI A	C.I.	81	1500	13.9	41.4
	C.I.	24	1900	.36	46.2
	C.I.	32	1800	32.76	48.7
	C.I. Blade	51	1700	0	$-\infty$
	C.I. Blade	13	2000	36.51	53.1
	C.I. Blade	32	1800	26.42	48.5
	C.I. Blade	64	1650	.57	41.7
	C.I. Blade	81	1500	4.15	40.4
IN 738	C.I.	18	1900	2.55	48.2
	C.I.	18	1900	5.51	49.0
	C.I.	41	1700	6.51	45.0
	C.I.	41	1700	8.27	45.2
	C.I. Blade	26	1800	16.52	48.0
	C.I. Blade	26	1800	13.39	47.7
	C.I. Blade	37	1700	17.51	45.9
	C.I. Blade	37	1700	14.95	45.7
	C.I. Blade	51	1600	28.92	44.3
	C.I. Blade	51	1600	5.11	42.7
	C.I. Blade	76	1500	18.56	41.7
	C.I. Blade	76	1500	10.34	41.2
Mar M 302	C.I.	12.5	1900	8.91	49.5
	C.I.	12.5	1900	19.03	50.2
	C.I.	24	1700	12.18	45.6
	C.I.	40	1700	.51	42.6
	ZRBSC	6	2000	46.98	53.3
	ZRBSC	16	1800	138.66	50.0
	ZRBSC	40	1530	73.05	43.5
Mar M 509	C.I. Blade	8	2000	13.84	52.0
	C.I. Blade	17	1800	64.45	49.3
	C.I. Blade	33	1590	44.19	44.4
	C.I. Blade	39	1500	90.17	43.0
304 Stainless Conventional	C.I. Blade	10	1325	956.13	41.0
	C.I. Blade	10	1325	360.61	40.3
	C.I. Blade	20	1170	215.89	36.7
	C.I. Blade	20	1170	21.23	34.7
304 Stainless Rheocast	C.I. Blade	10	1325	905.18	41.0
	C.I. Blade	10	1325	235.49	40.0
	C.I. Blade	20	1170	495.65	37.0
	C.I. Blade	20	1170	75.59	35.6

TABLE V (continued)

	Mold	σ(ksi)	T(°F)	Life (hours)	P_{20}
Modified TRW Vla	C.I.	13	2000	.71	48.8
	C.I.	32	1800	16.55	47.9
	C.I.	32	1800	.63	44.7
	C.I.	46	1700	8.44	45.2
	C.I.	62	1600	2.08	41.9
	C.I.	81	1500	.27	38.1
	C.I.	81	1500	4.25	40.5
Modified IN 738	C.I.	15	1900	9.33	49.5
	C.I.	26	1800	7.80	47.3
	C.I.	26	1800	4.35	46.1
	C.I.	36	1700	14.19	45.7
	C.I.	54	1600	9.30	43.2
	C.I.	54	1600	10.51	43.3
	C.I.	75	1500	6.38	40.7

TABLE VI

	Mold	Y.S. (ksi)	U.T.S. (ksi)	%El.	T(°F)
304 Stainless Conventional	C.I. Blade	34.9	116	49.2	74
	C.I. Blade	31.5	118	47.2	74
	C.I. Blade	22.6	58.1	37.0	800
	C.I. Blade	23.5	56.1	33.8	800
304 Stainless Rheocast	C.I. Blade	27.6	109	33.4	74
	C.I. Blade	31.9	109	38.0	74
	C.I. Blade	24.4	57.5	32.4	800
	C.I. Blade	23.1	46.9	17.8	800
4340 Conventional	C.I. Blade	99.8	134.8	12.0	74
	C.I. Blade	108.8	135.0	10.7	74
4340 Rheocast	C.I. Blade	107.2	135.6	9.8	74
	C.I. Blade	114.2	140.6	10.3	74

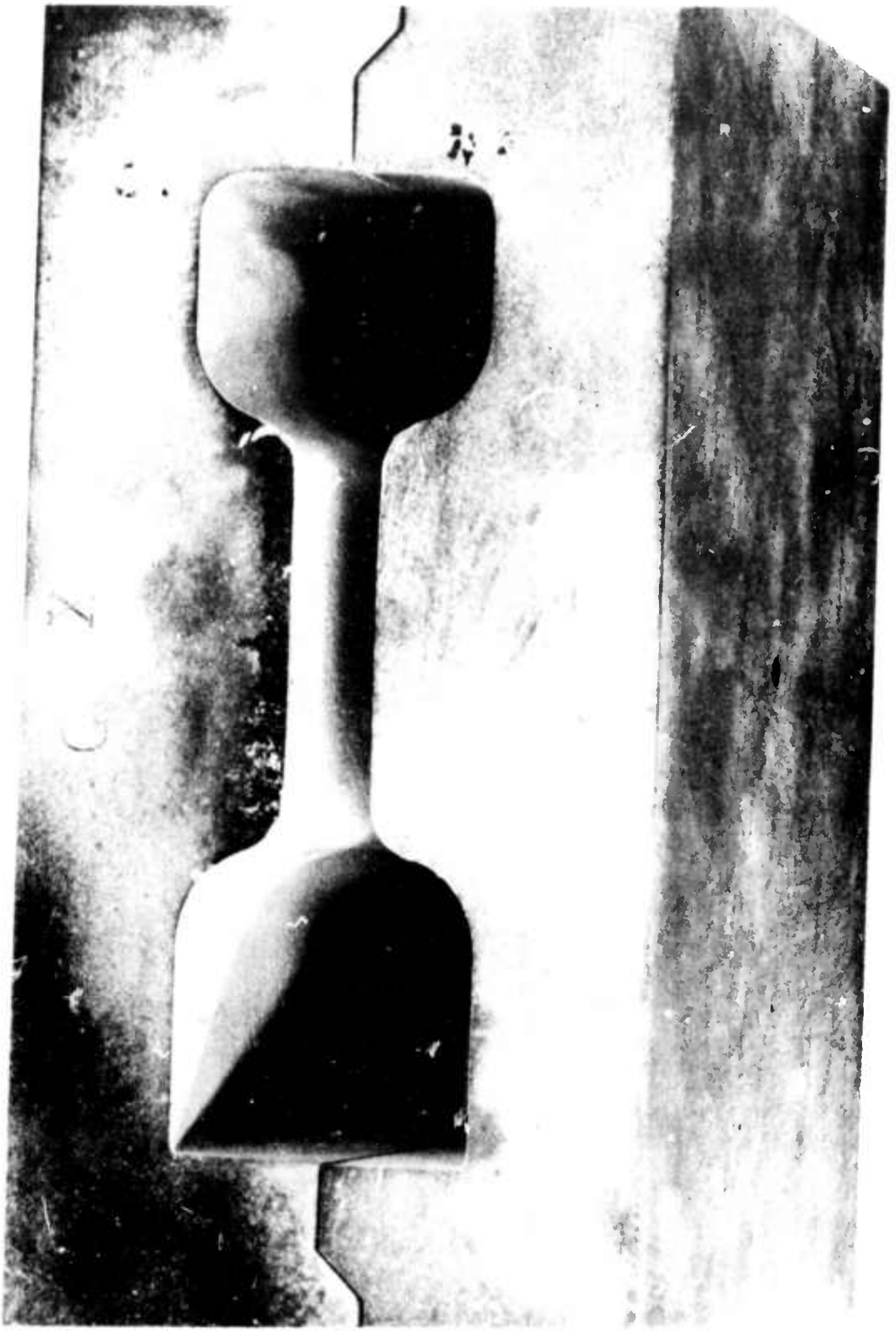

Figure 1. Grey iron mold. Cavity is 5 inches long, and web is 1/2 inch thick.

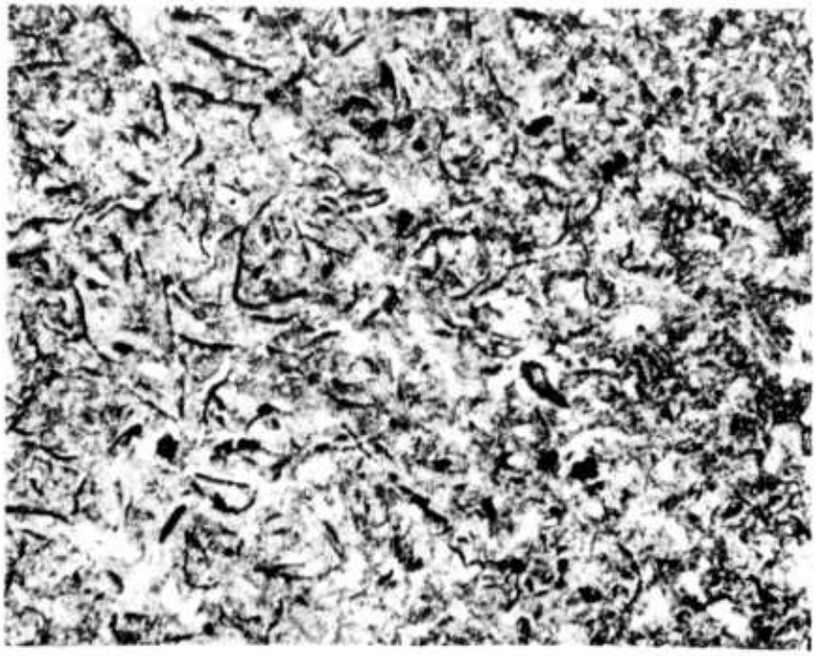

Figure 2. Grey iron microstructure: flake graphite, pearlite and carbides. 100X

Figure 3. Pouring basin. Basin is "vee" shaped with a slit opening in bottom, the width of the mold cavity. It is made of high fired zircon.

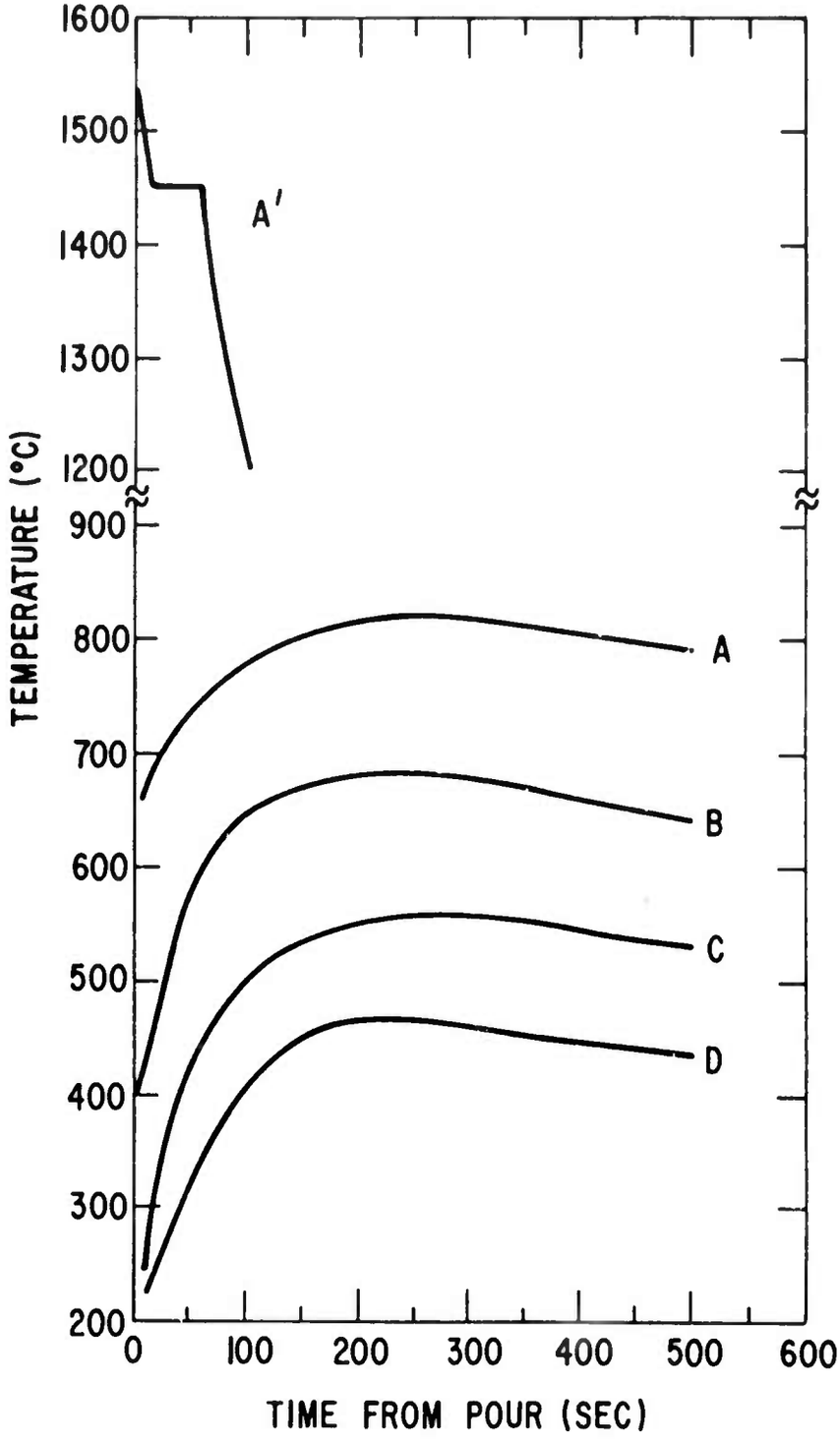

Figure 4. Thermal behavior of all metal molds. A'-304 stainless casting, 630°C mold; A-mold web, 304 stainless casting, 1550°C pouring; B-mold web, IN-738 casting, 1470°C pouring; C-mold web, IN-738 casting, 1470°C pouring; D-mold end, IN-738 casting, 1420°C pouring.

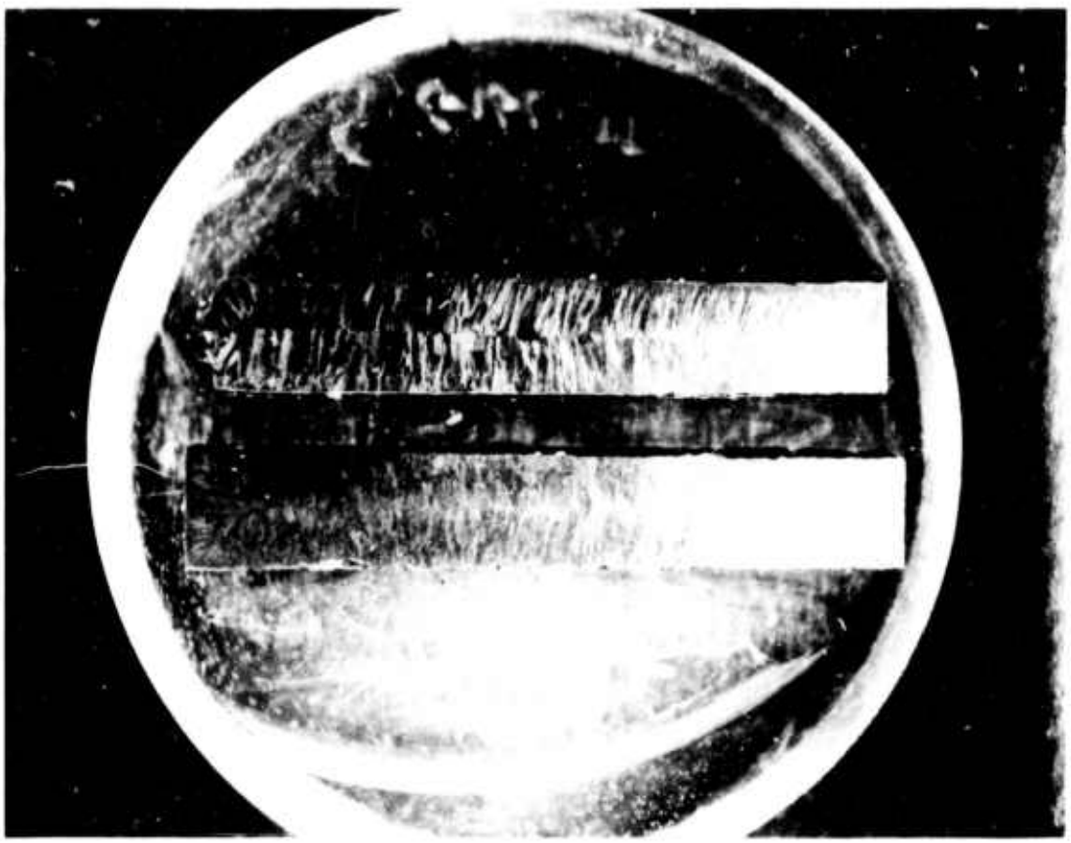

Figure 5. IN-738 casting, web section. Mold temperature 200°C, superheat 50°C. Hot tear in lower right of picture. Lower left is bottom of casting, upper left is top of casting. 1.25X.

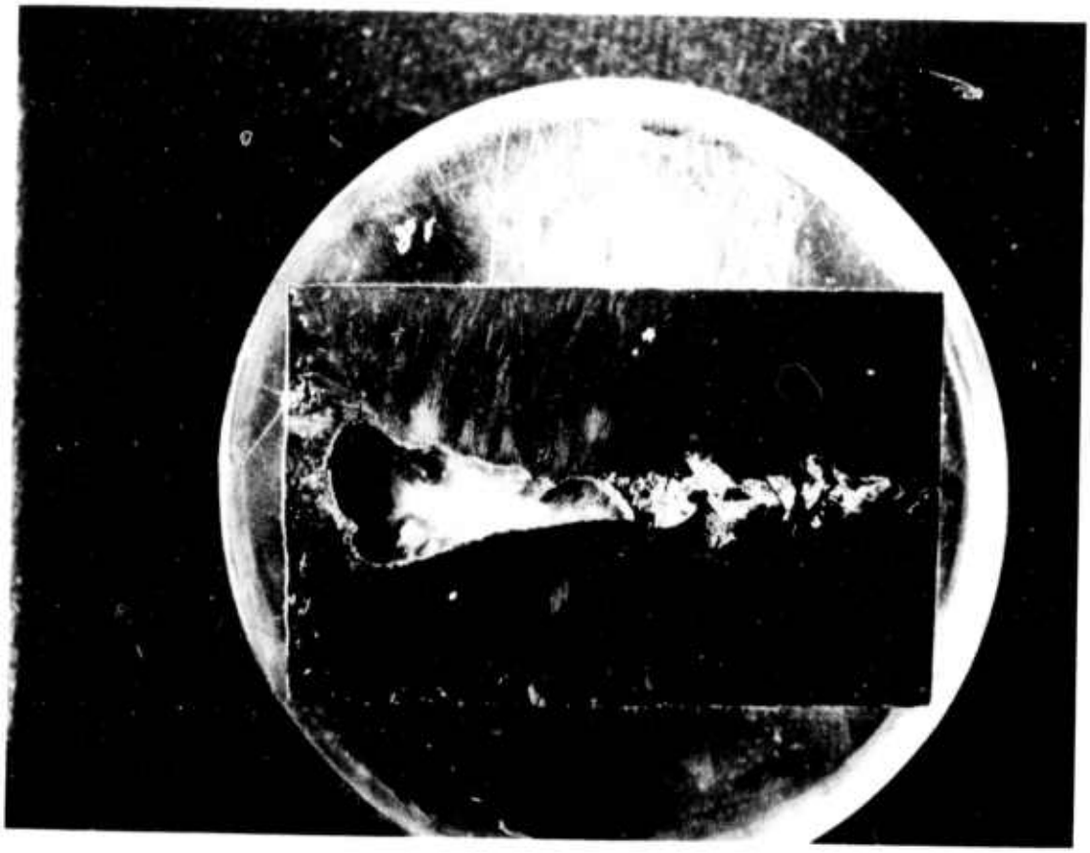

Figure 6. IN-738 casting poured into 200°C mold. Metal superheat was 100°C. Micrograph shows upper half of thick section. Gross porosity present to within 1 inch from bottom. 1.25 X.

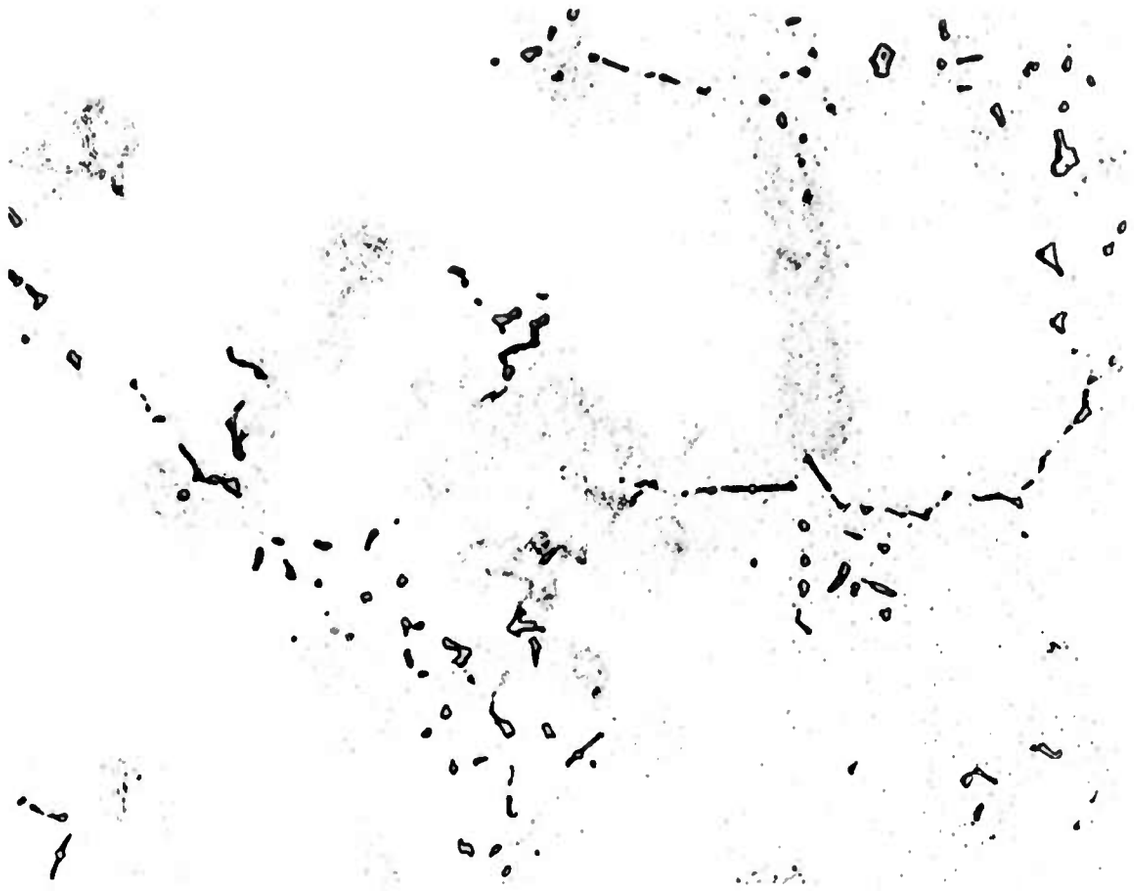

Figure 7. IN-738 casting, center of thick section shown in Fig. 4. Only slight amounts of γ-γ' eutectic present. 750X.

Figure 8. IN-738 center of web section, same casting as in Fig. 5. Etched with Marble's reagent, shows no centerline porosity. 150X.

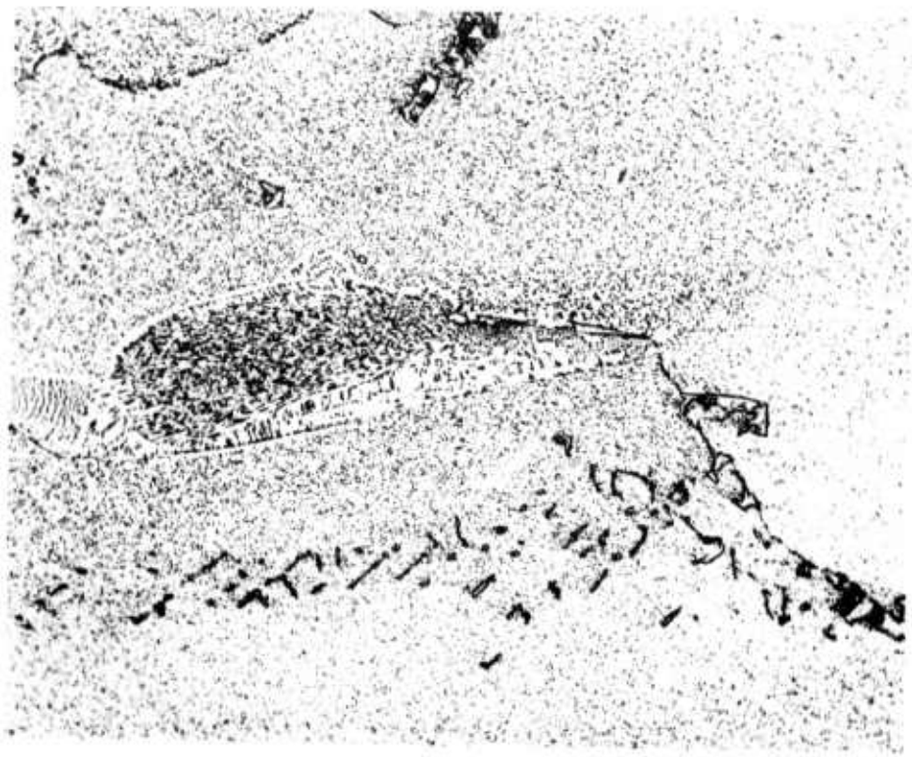

Figure 9. IN-738 grown at 1/4"/hr. Growth axis horizontal. $\gamma - \gamma'$ segregate in center of photograph. 250X

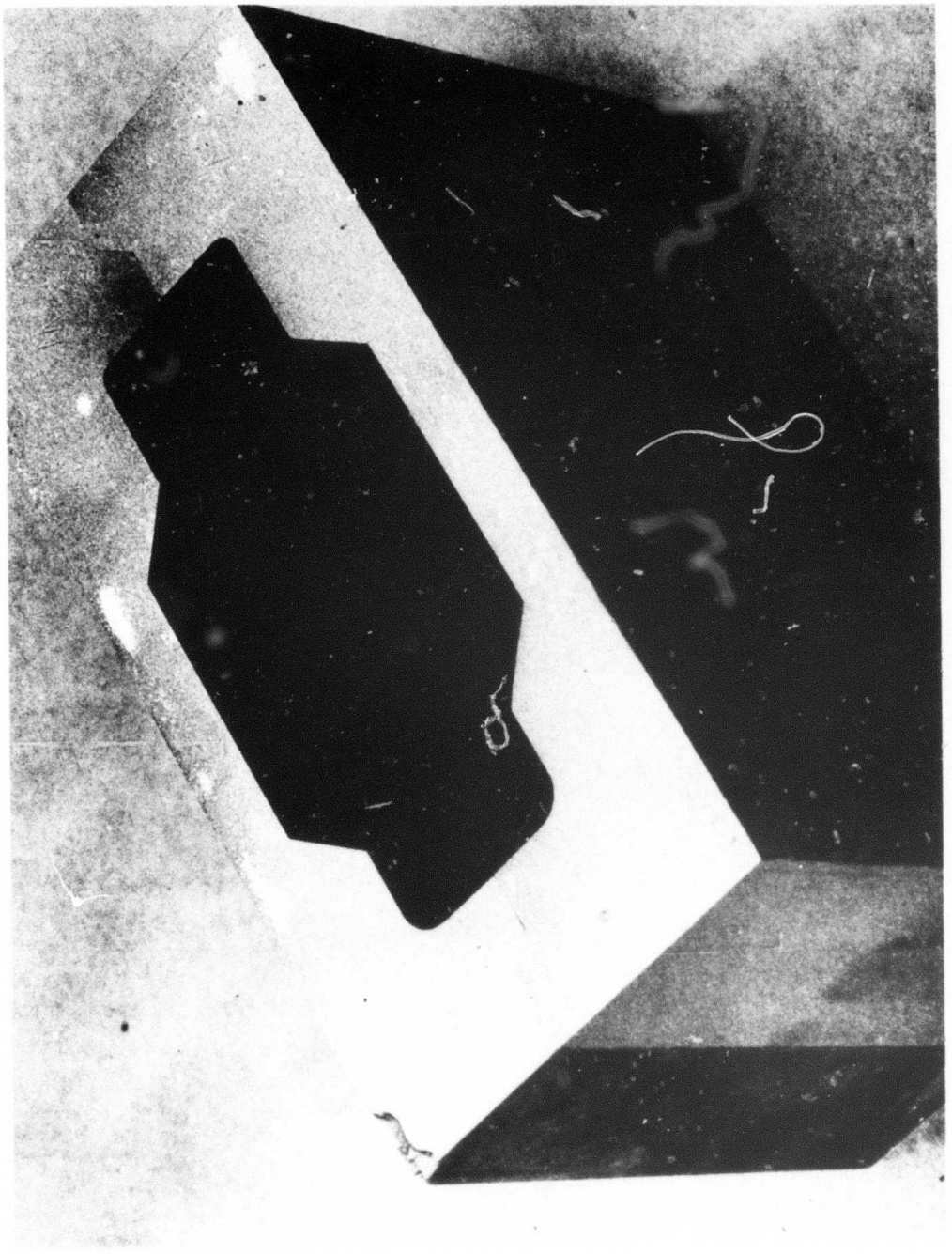

Figure 10. Grey iron permanent mold for inserts. Thick sections of casting shape same as in Fig 1.

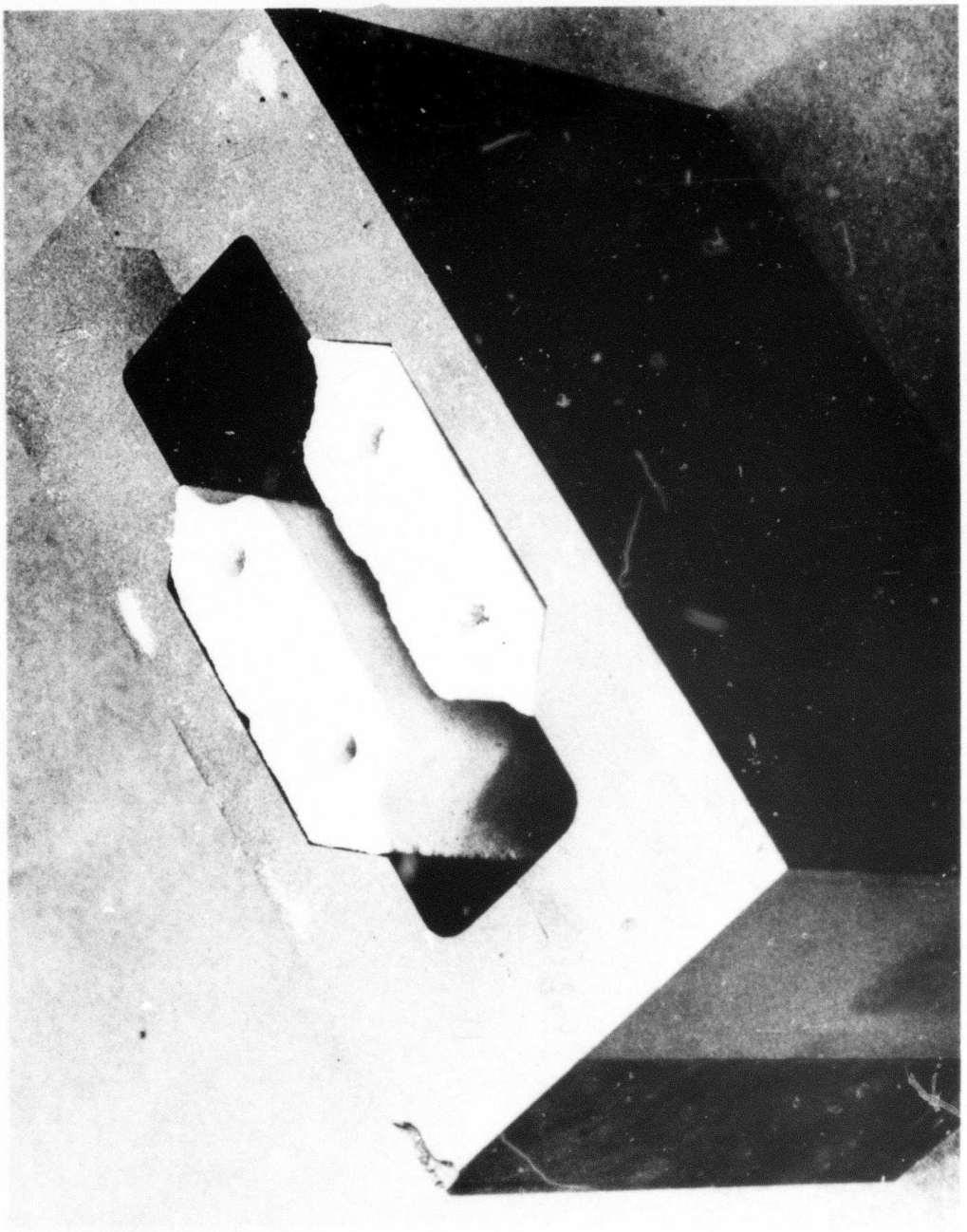

Figure 11. Grey iron mold with inserts in place. Inserts are designed to collapse and thus prevent hot tearing.

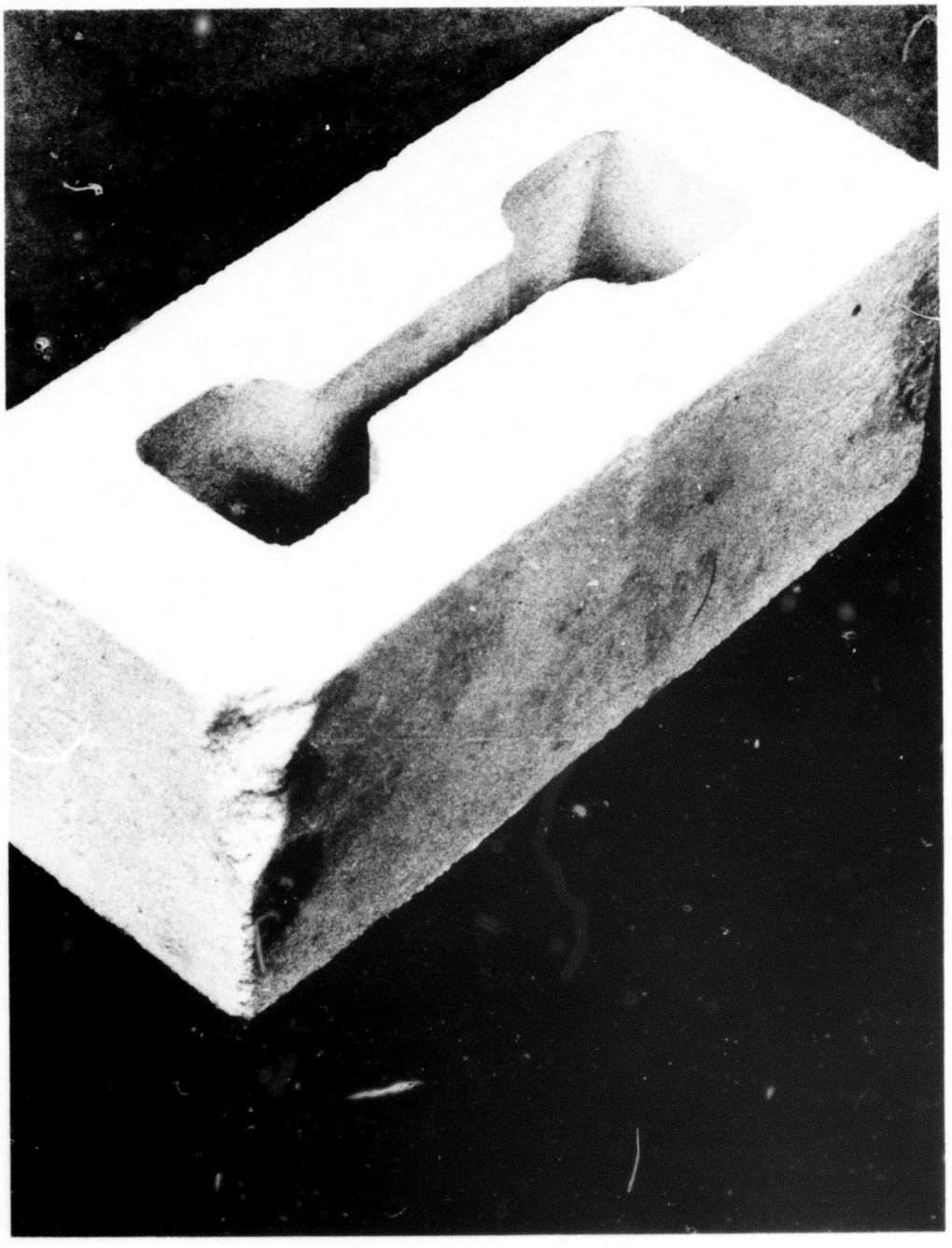

Figure 12. Ceramic Riser configuration on top of permanent mold.

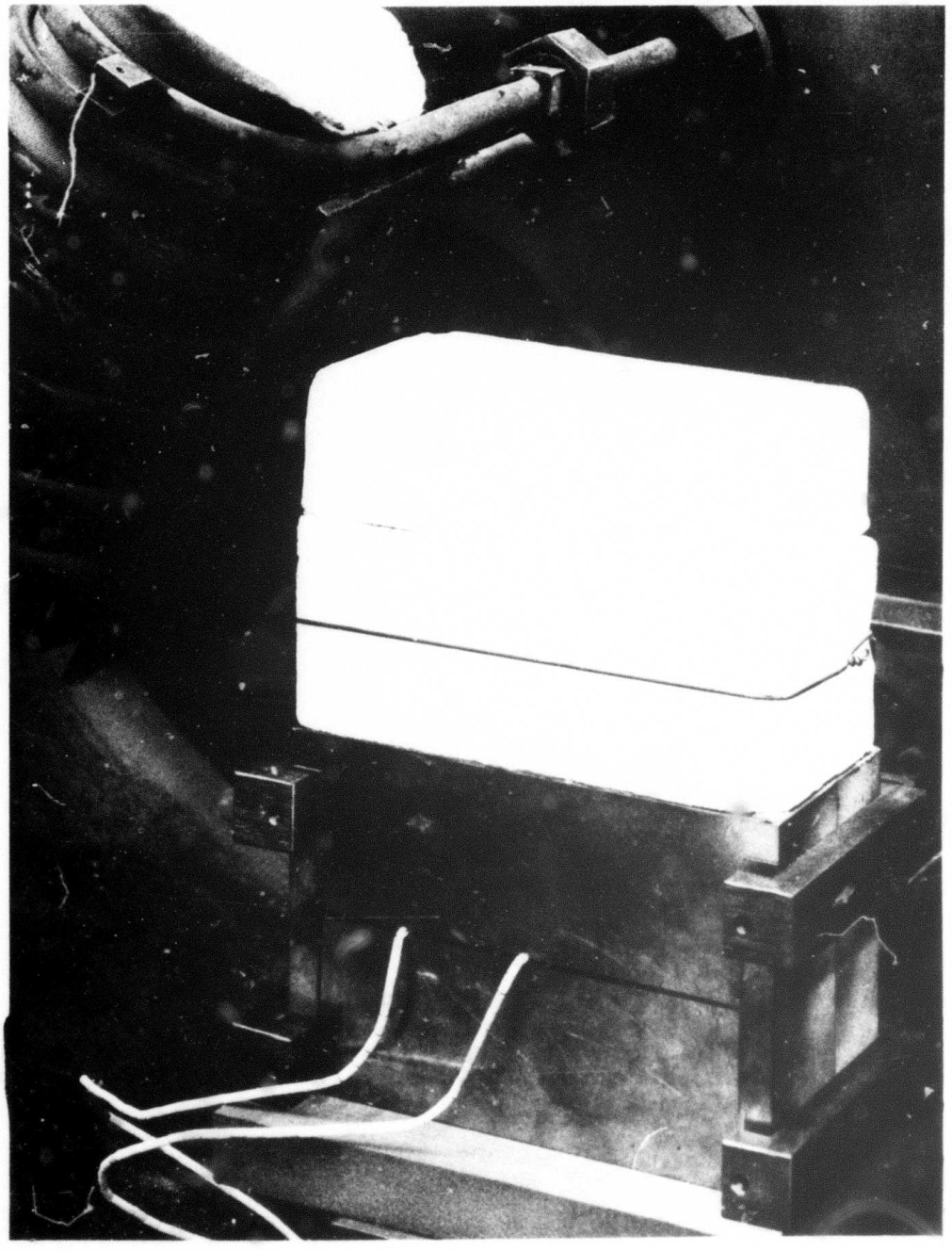

Figure 13. Furnace arrangement: mold, pouring basin, and riser. Thermocouples extending out of mold monitor melt temperature, mold temperature, and insert temperature. Mold arrangement is surrounded by heater in actual use.

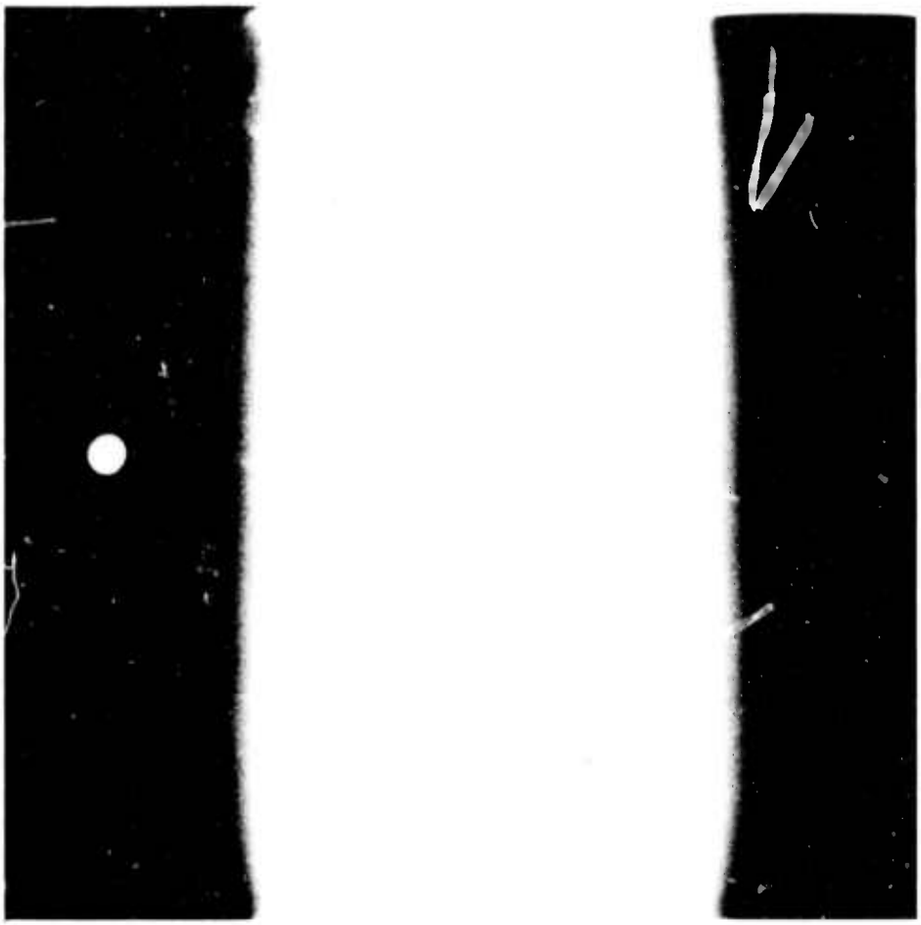

Figure 14. X-ray photograph of Mar M-302 casting made with riser arrangement of Fig. 13. 1430°C pouring temperature, 400°C mold temperature. Hole in center left is thermocouple tube. Only slight porosity present, in upper left, next to web.

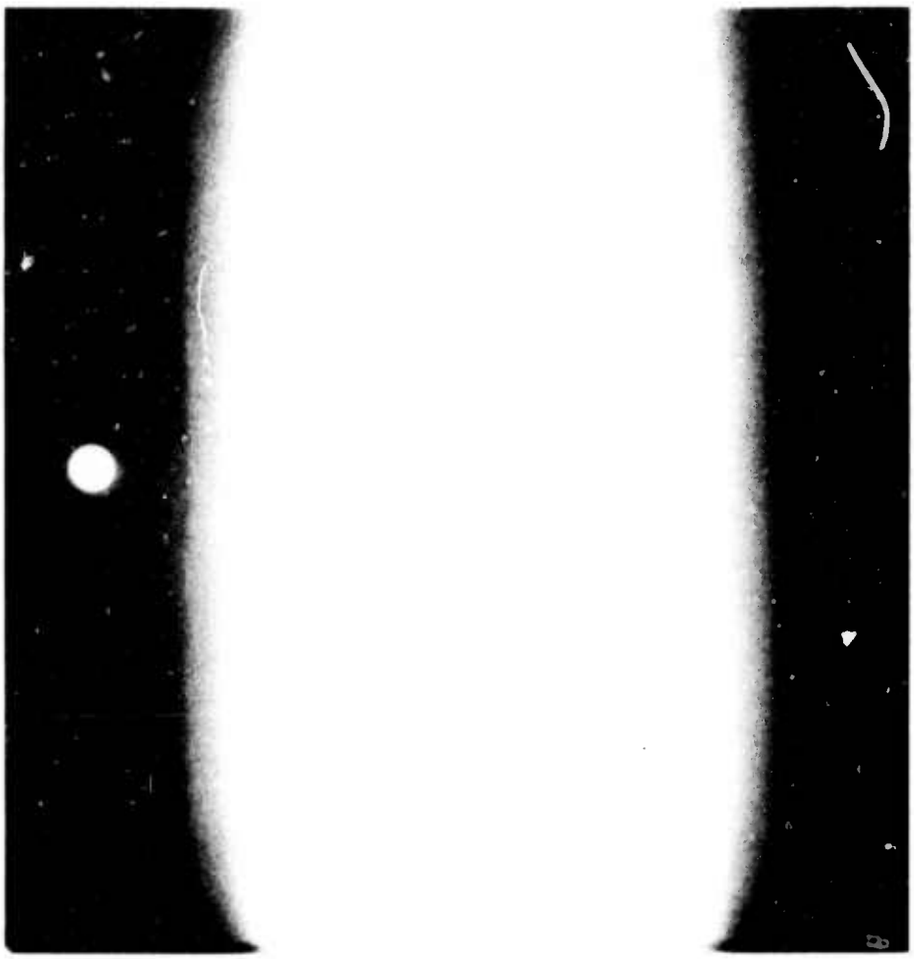

Figure 15. X-ray photograph of IN-738 casting made as in Fig. 13. 1470°C pouring temperature, 400°C mold temperature. Hole in center left is thermocouple tube. Surface defects visible as small circles. No porosity evident.

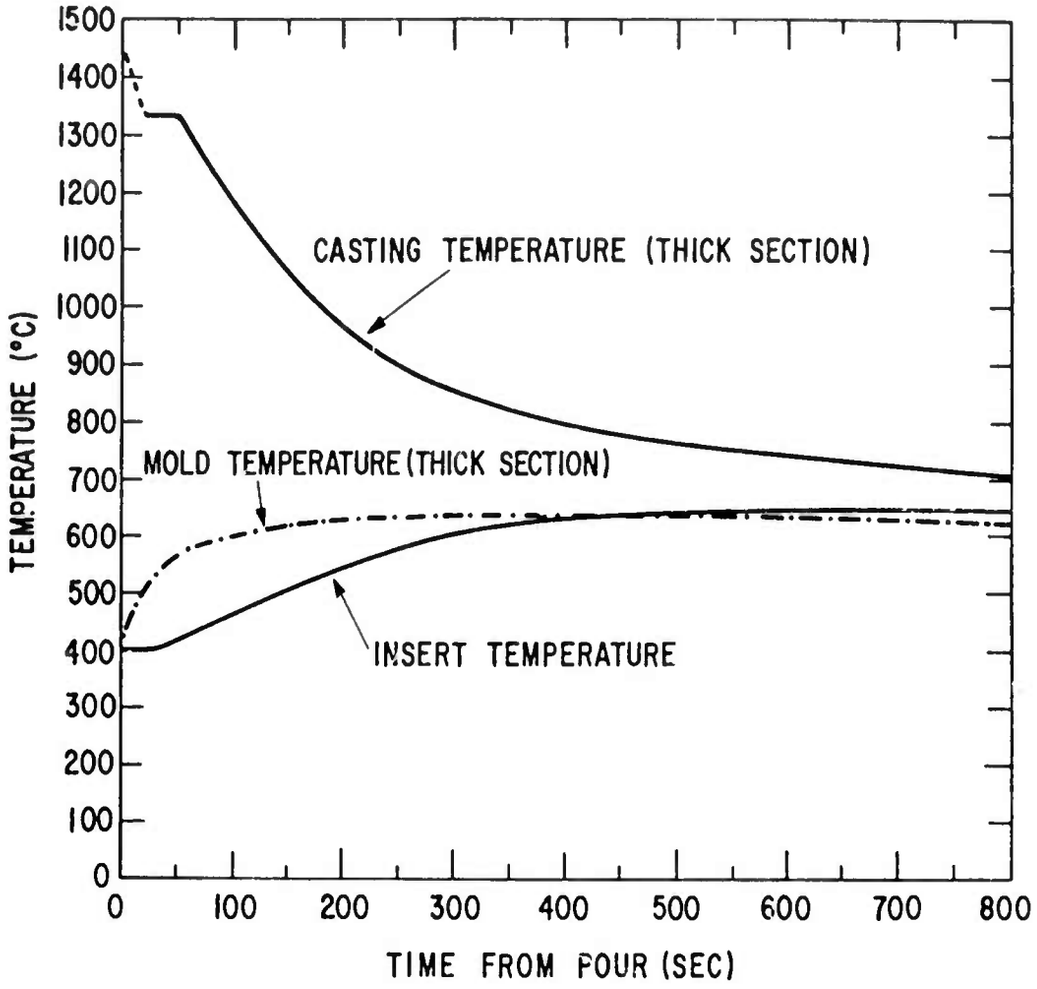

Figure 16. Thermocouple data showing casting temperature, mold temperature, and temperature of insert. Alloy cast was Mar M-302, mold temperature 400°C, pouring temperature 1435°C.

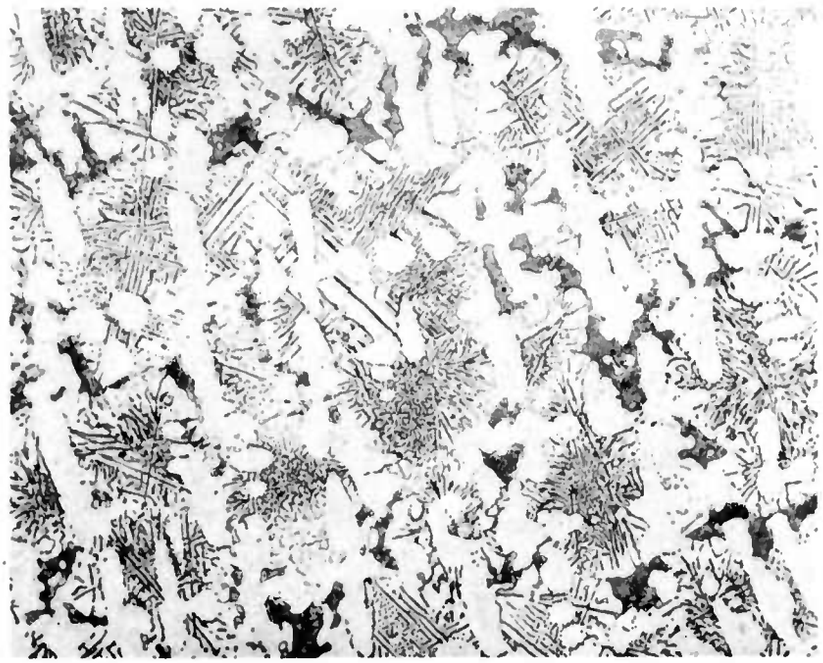

Figure 17. Mar M-302 cast at 1430°C, 400°C mold temperature. Center of thick section of casting. Co-base dendrites, script MC carbide, M_6C-$M_{23}C_6$ eutectic (grey phase). Marble's reagent. 250X

Figure 18. Same casting as Fig. 17. Center of web section. Coarser structure than Fig. 17. Marble's reagent. 250X

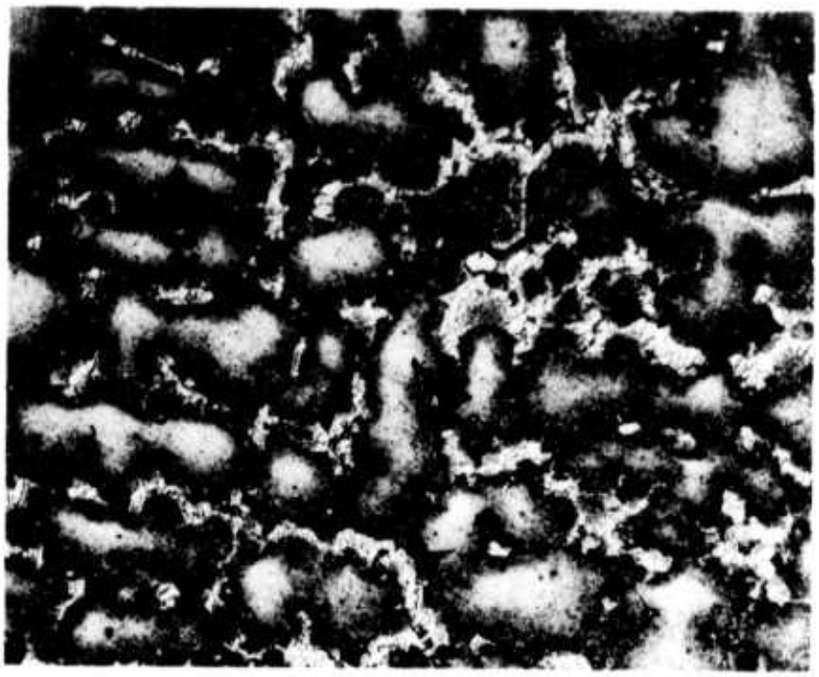

Figure 19. TRW VI A cast in permanent mold at 1430°C and 400°C mold temp. Center of thick section of casting. Ni-base dendrites surrounded by network of $\gamma - \gamma'$ eutectic. Porosity associated with eutectic in lower center. Marble's reagent. 250X

Figure 20. TRW VI A casting same as Fig. 19. Center of web section. Same features as thick section except coarser microstructure. Porosity associated with $\gamma - \gamma'$ eutectic in lower right. Marble's reagent. 250X

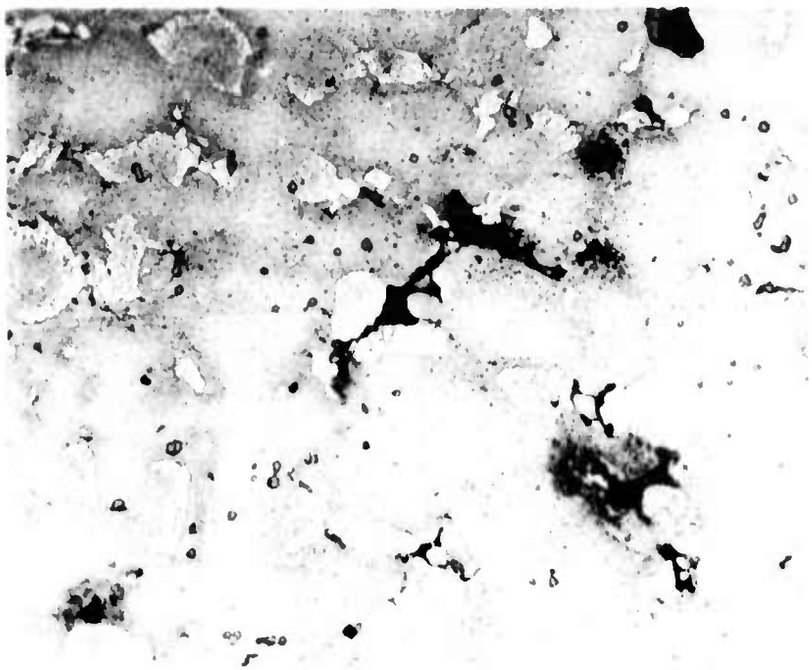

Figure 21. TRW VI A casting same as Figs. 19 and 20. Microporosity associated with γ - γ' eutectic. Marble's reagent. 250X

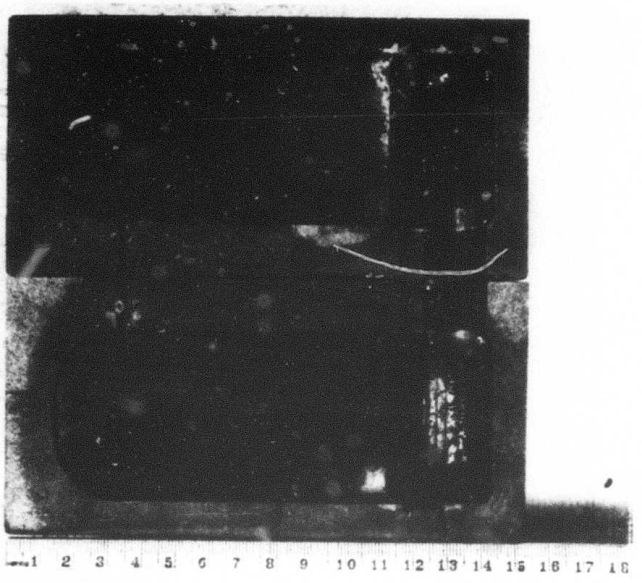

Figure 22. Blade shape mold machined from block of ZRBSC-M(R). Mold has cracks in root section which occurred during pouring.

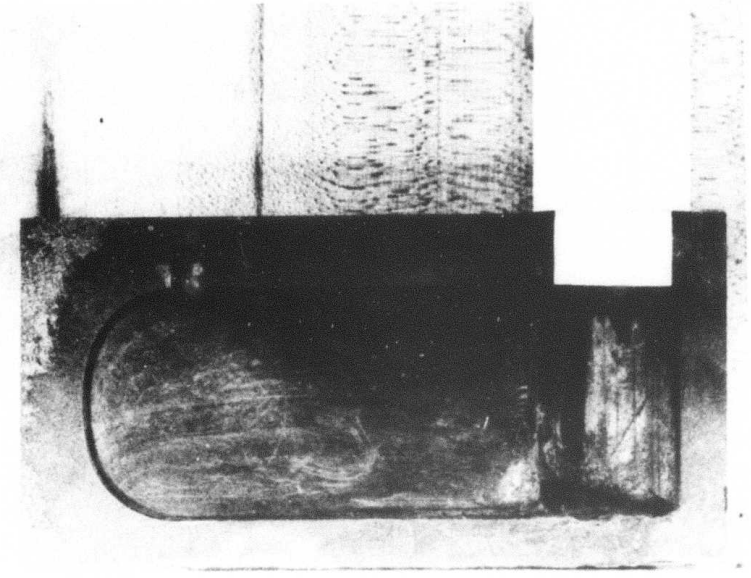

Figure 23. Blade mold with alumina insert tubes. Cracks repaired with powdered graphite and potassium silicate.

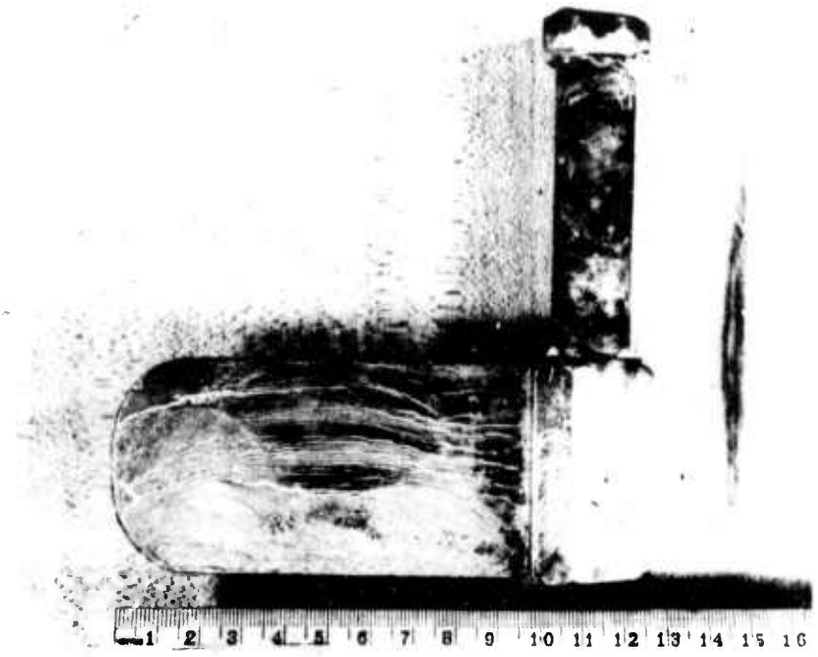

Figure 24. Mar M-302 blade shape casting. Poured at 1430°C, 550°C mold temperature. Ceramic tube removed.

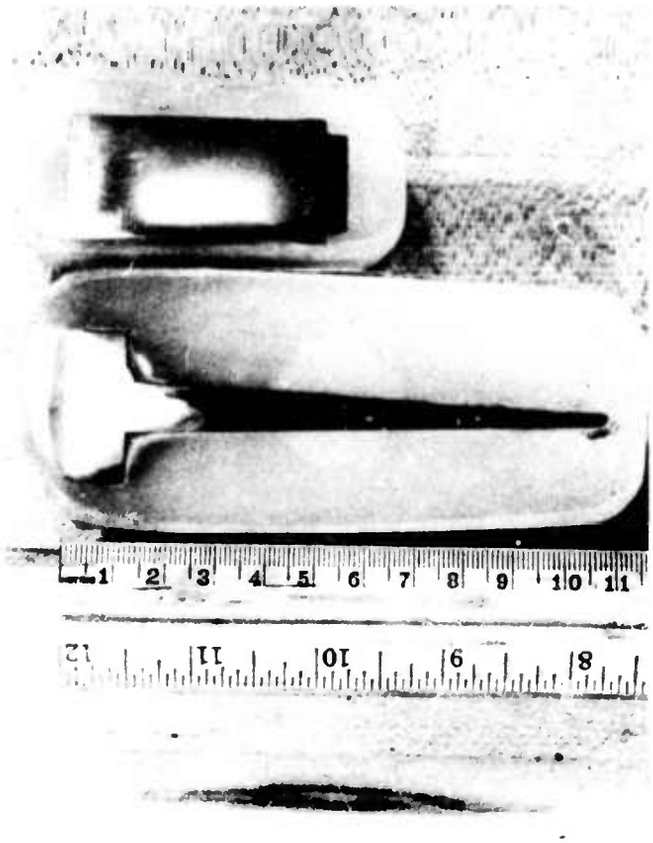

Figure 25. Cross sections of casting shown in Fig. 24. No gross porosity visible. Upper section is midplane of root section. Lower section is midplane through blade. Riser not shown.

Figure 26. Microstructure of blade casting shown in Fig. 24. Structure is finer than that in Figs. 17 and 18. No porosity evident. Marble's reagent. 250X

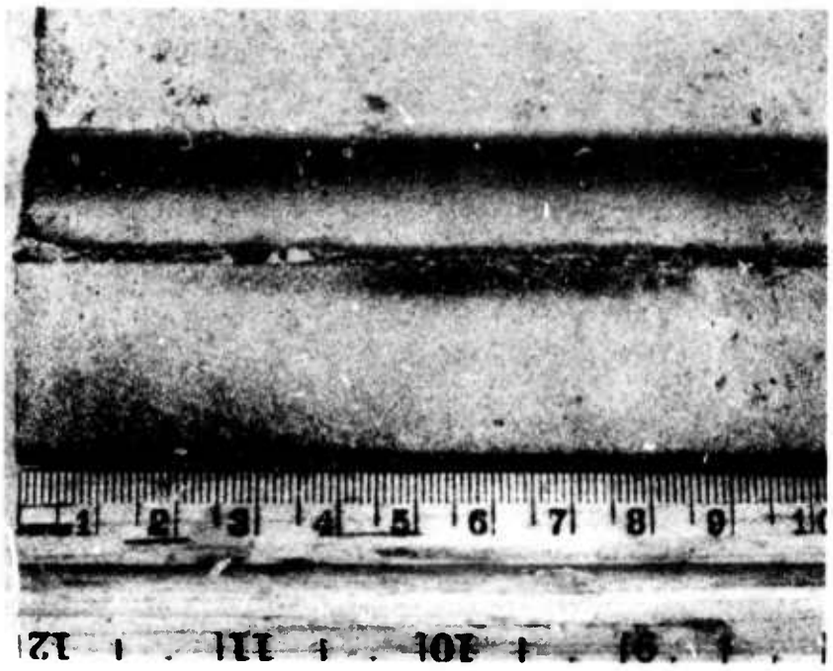

Figure 27. Surface finish of IN-738 casting made in mold plasma sprayed with ZrO_2. Mold had high-fired zircon inserts.

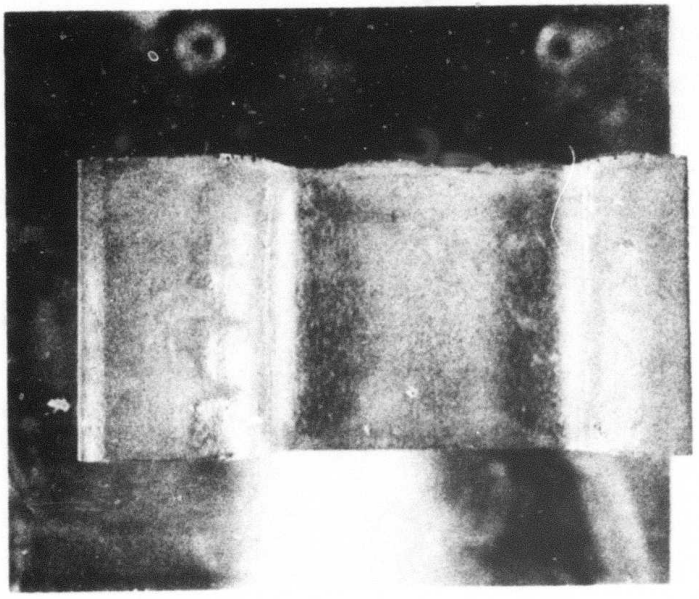

Figure 28. Surface finish of 304 stainless casting made in mold plasma sprayed with ZrO_2. 1450°C pouring temperature, 600°C mold temperature, all-metal mold.

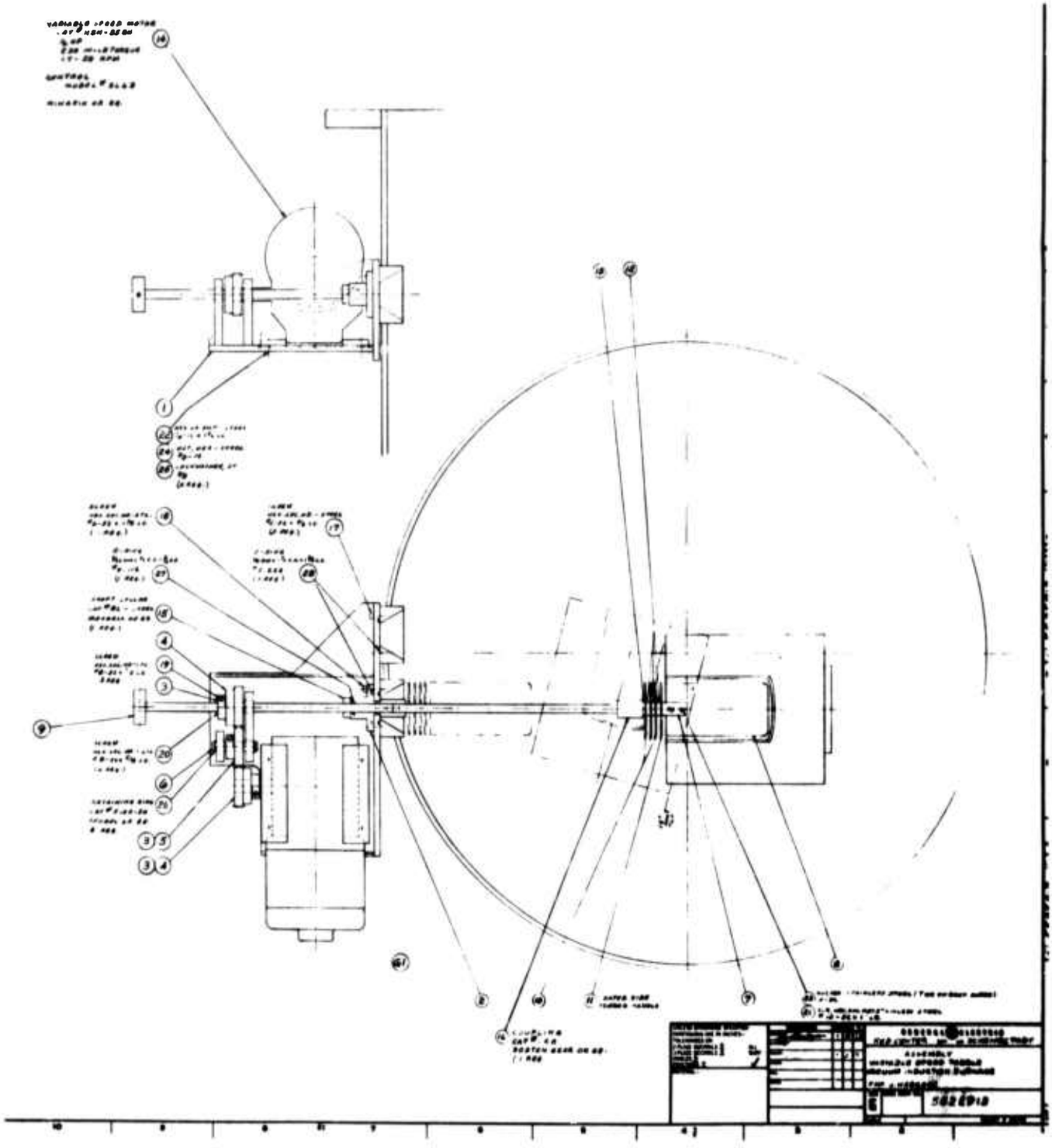

Figure 29. Schematic of rheocasting attachment for vacuum melting furnace. Motor and gear drive mount externally. Shaft enters through O ring seal. Paddles are alumina and plasma sprayed molybdenum. There are Ta shields above paddle. Shaft with paddle can be retracted to permit pouring.

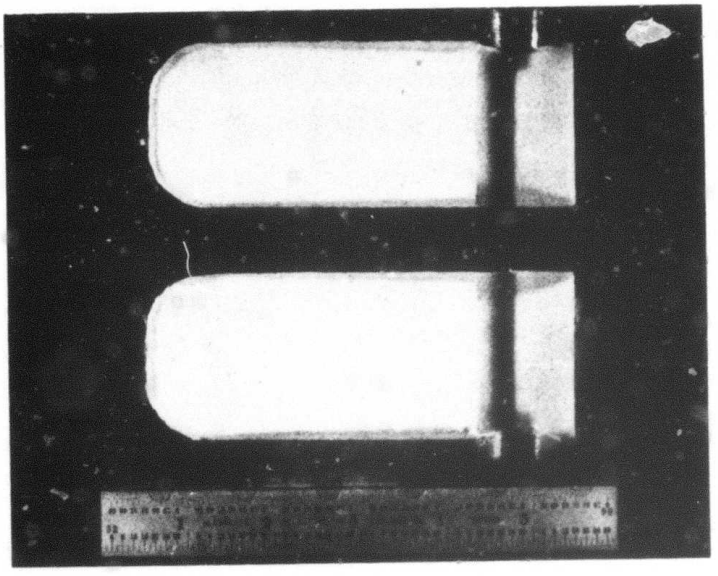

Figure 30. Austenitic grey iron mold. Mold is identical in shape to that in Fig. 22. Interior of mold plasma-sprayed with ZrO_2.

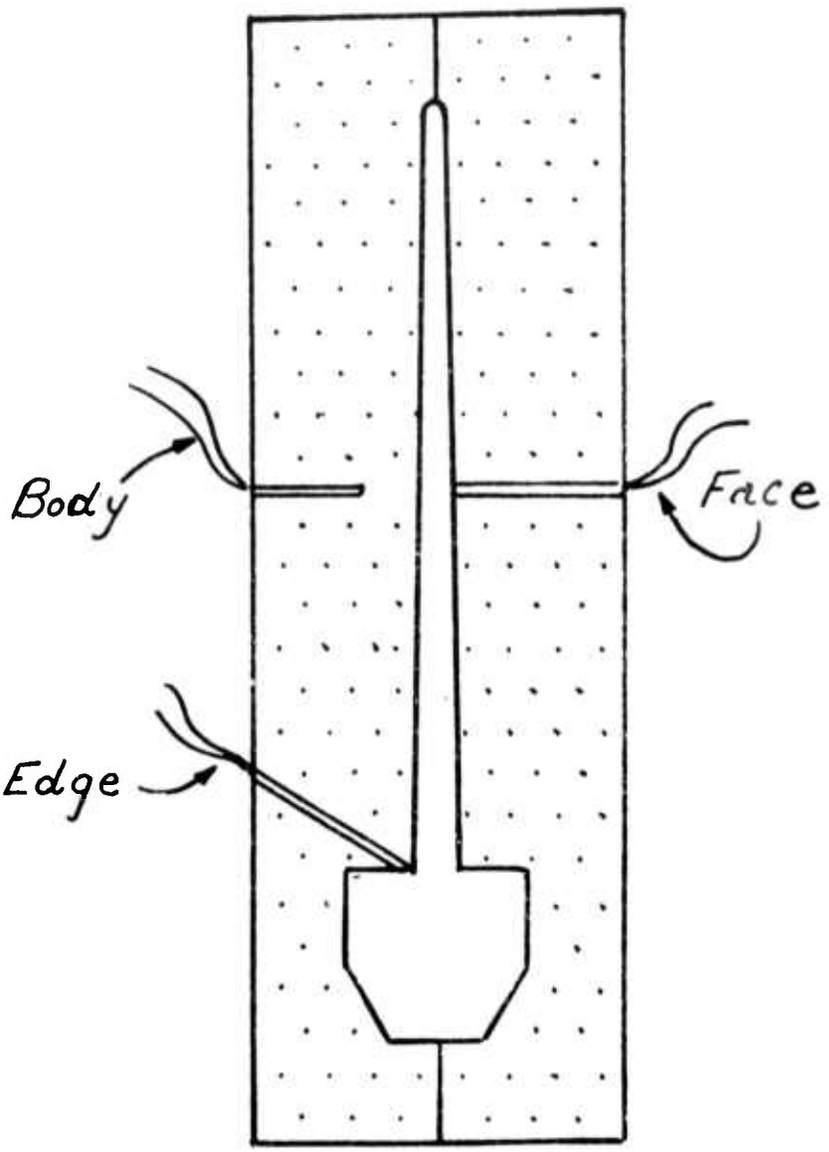

Figure 31. Schematic of grey iron blade mold showing position of thermocouples. Thermocouples on face and edge positions welded to inside mold face.

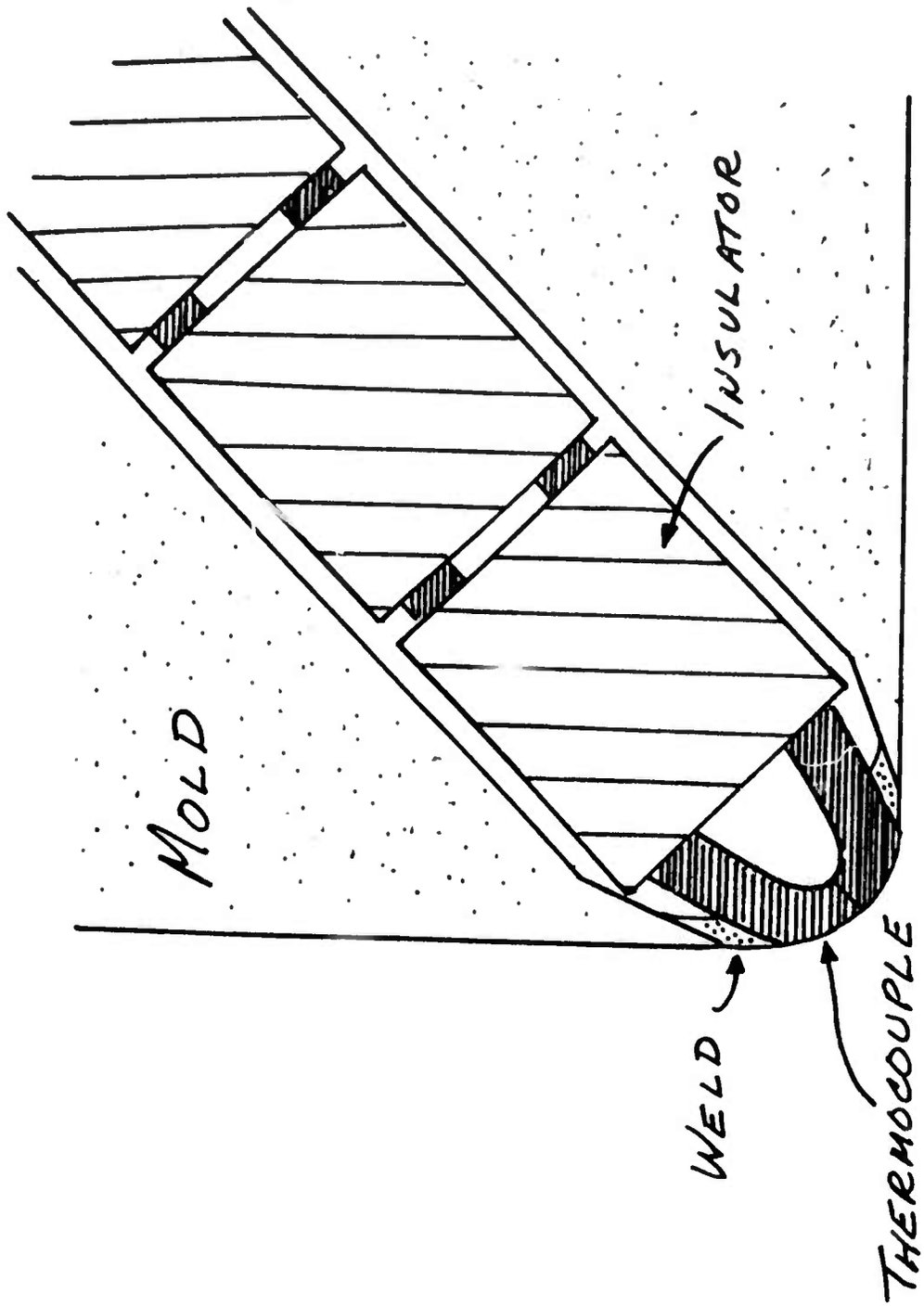

Figure 32. Schematic of thermocouple in edge position on mold. Thermocouple is welded onto face. Hole for thermocouple.

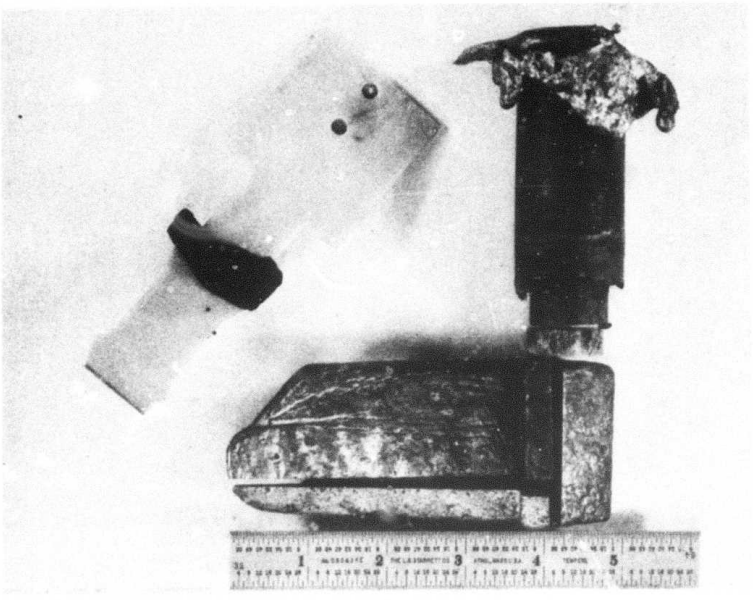

Figure 33. Alumina paddle and rheocasting. Paddle cracked during stirring. Casting did not fill, probably due to poor stirring of melt.

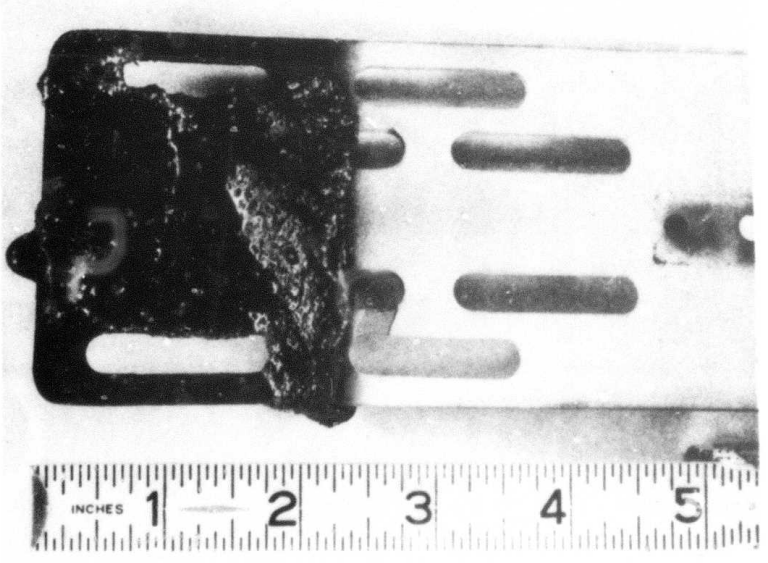

Figure 34. ZrO_2 sprayed molybdenum paddle. Metal mechanically adhering, but no penetration of coating.

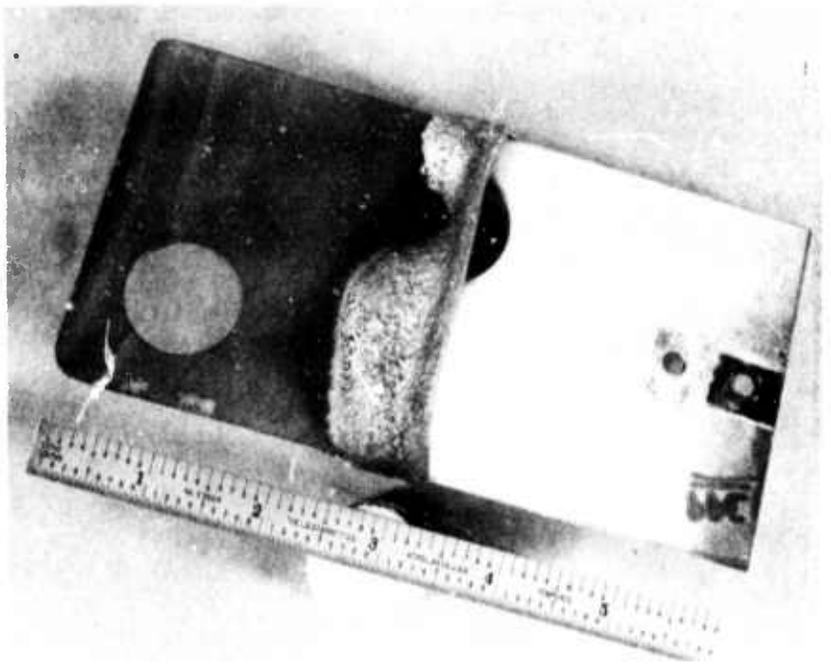

Figure 35. ZrO_2 sprayed molybdenum paddle. No metal penetration. Metal mechanically adhering.

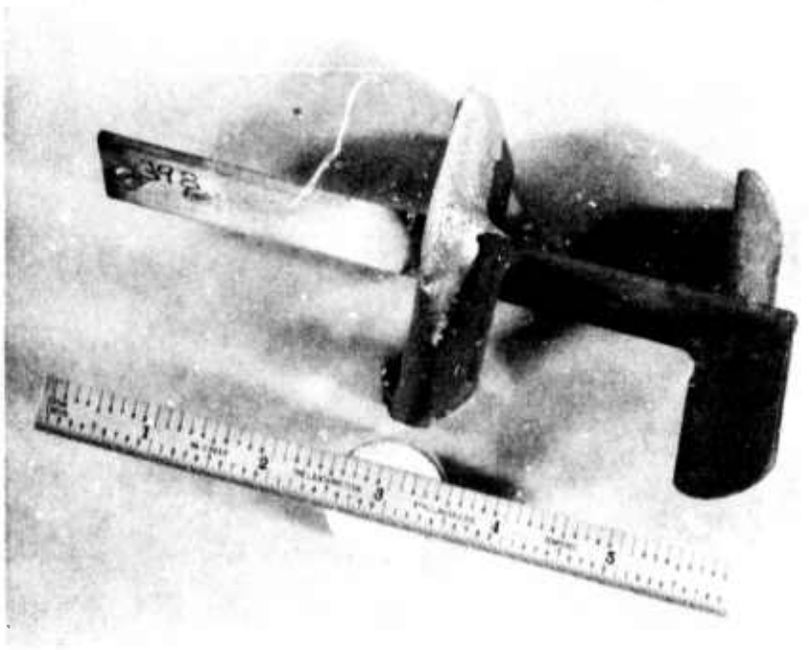

Figure 36. ZrO_2 sprayed molybdenum paddle. No metal penetration. Design prevents metal mechanically adhering to paddle.

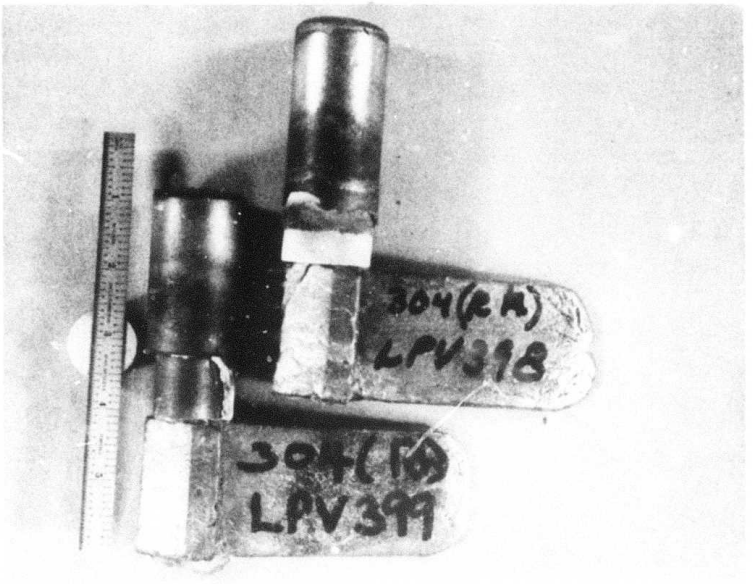

Figure 37. Rheocasting of 304 stainless steel.

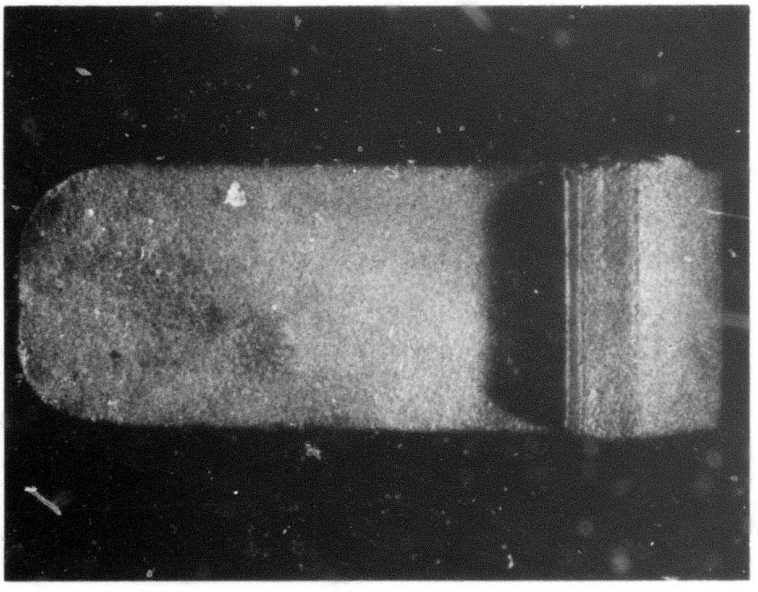

Figure 38. Conventional casting of 304 stainless steel.

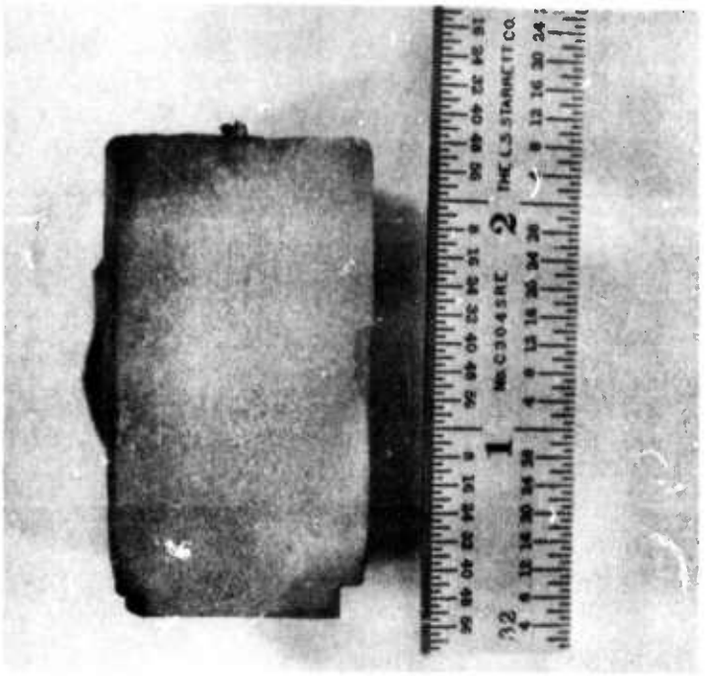

(a) rheocast

Figure 39. Grain size of IN 738 casting

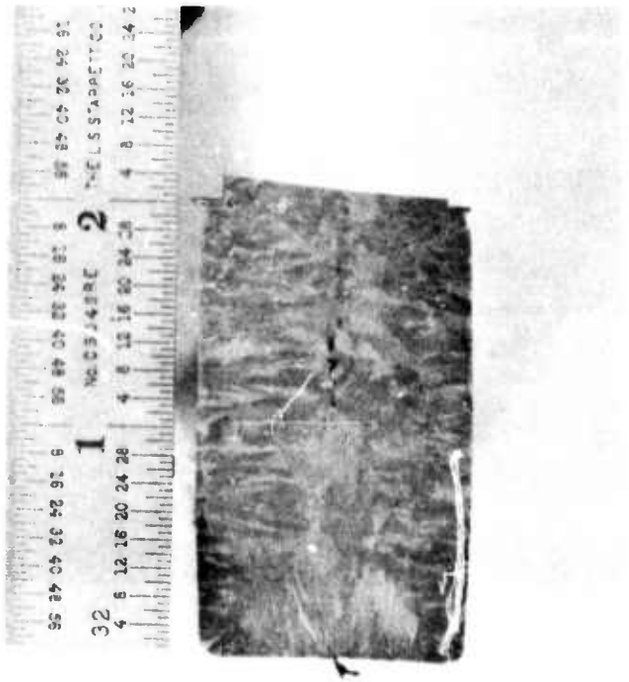

(b) conventional permanent mold cast

Figure 39 concluded

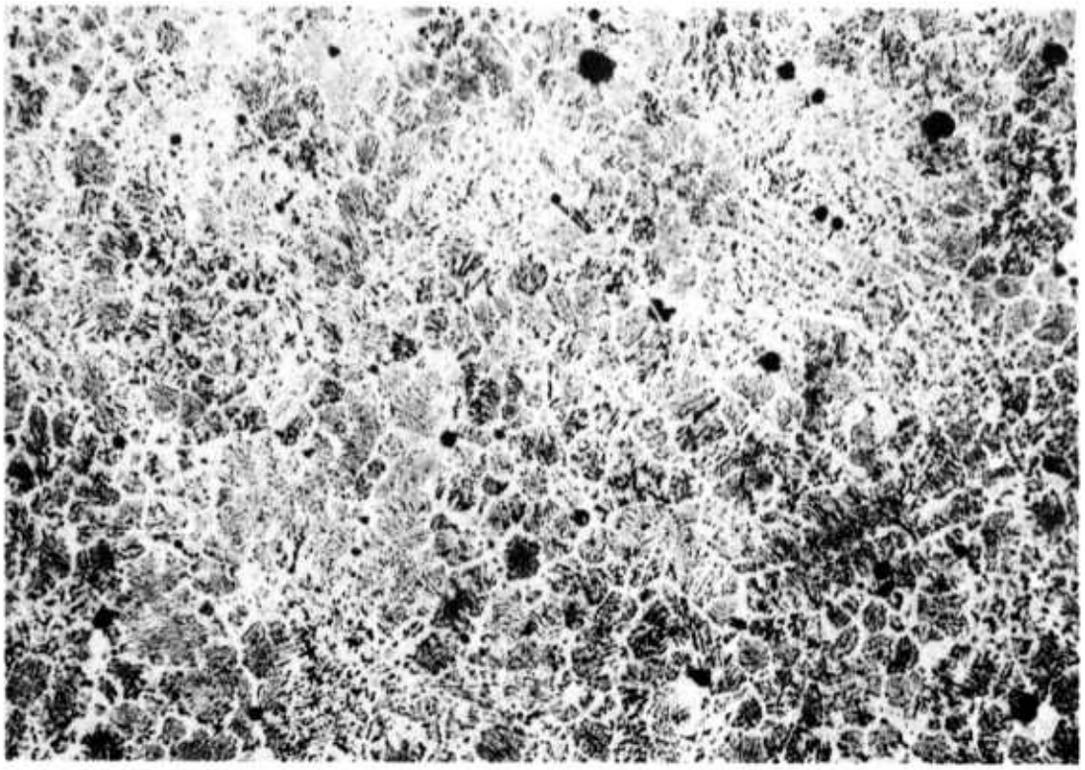

(a) rheocast 48X

Figure 40. Comparison of 304 stainless steel castings

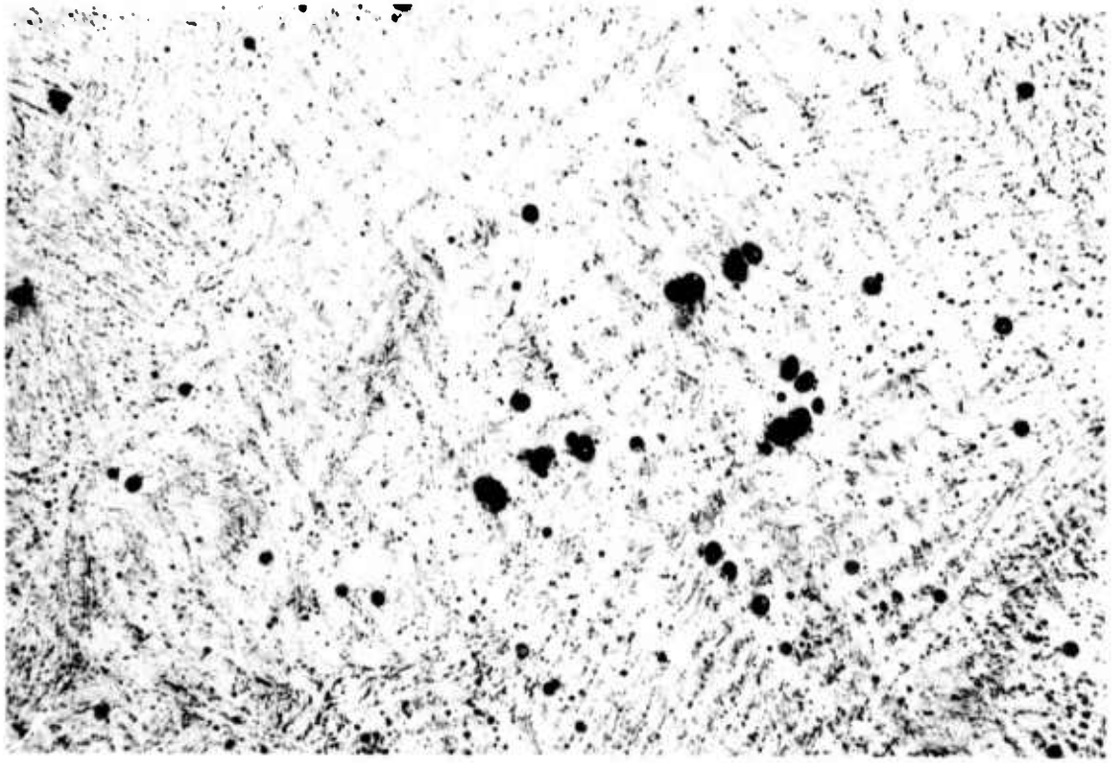

(b) conventional permanent mold cast 48X

Figure 40 concluded

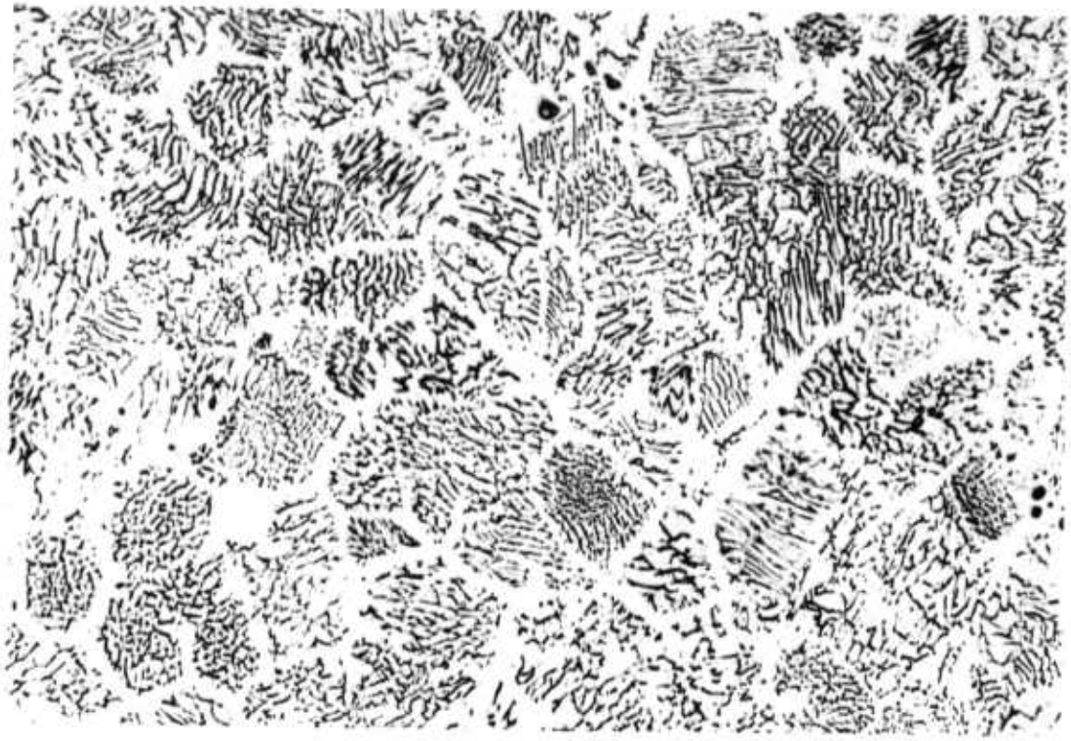

(a) rheocast 150X

Figure 41. Comparison of 304 stainless steel castings

(b) conventional permanent mold cast 150X

Figure 41 concluded

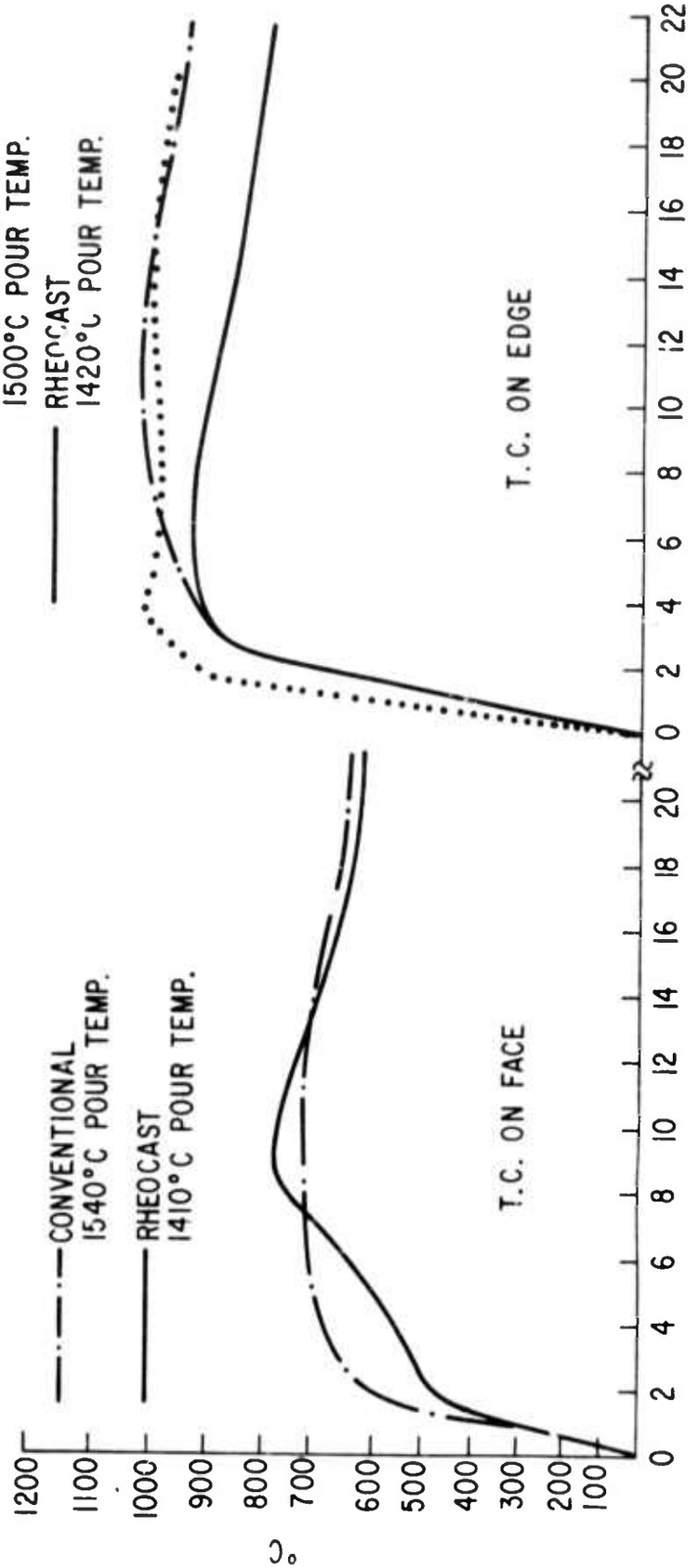

Figure 42. Mold face temperature response after casting. Face data may be affected by air gap formation as casting freezes.

Figure 43. Low B and Zr TRW VI A casting. $\gamma - \gamma'$ segregate eutectic is reduced in size and morphology changed. Marble's reagent. 250X

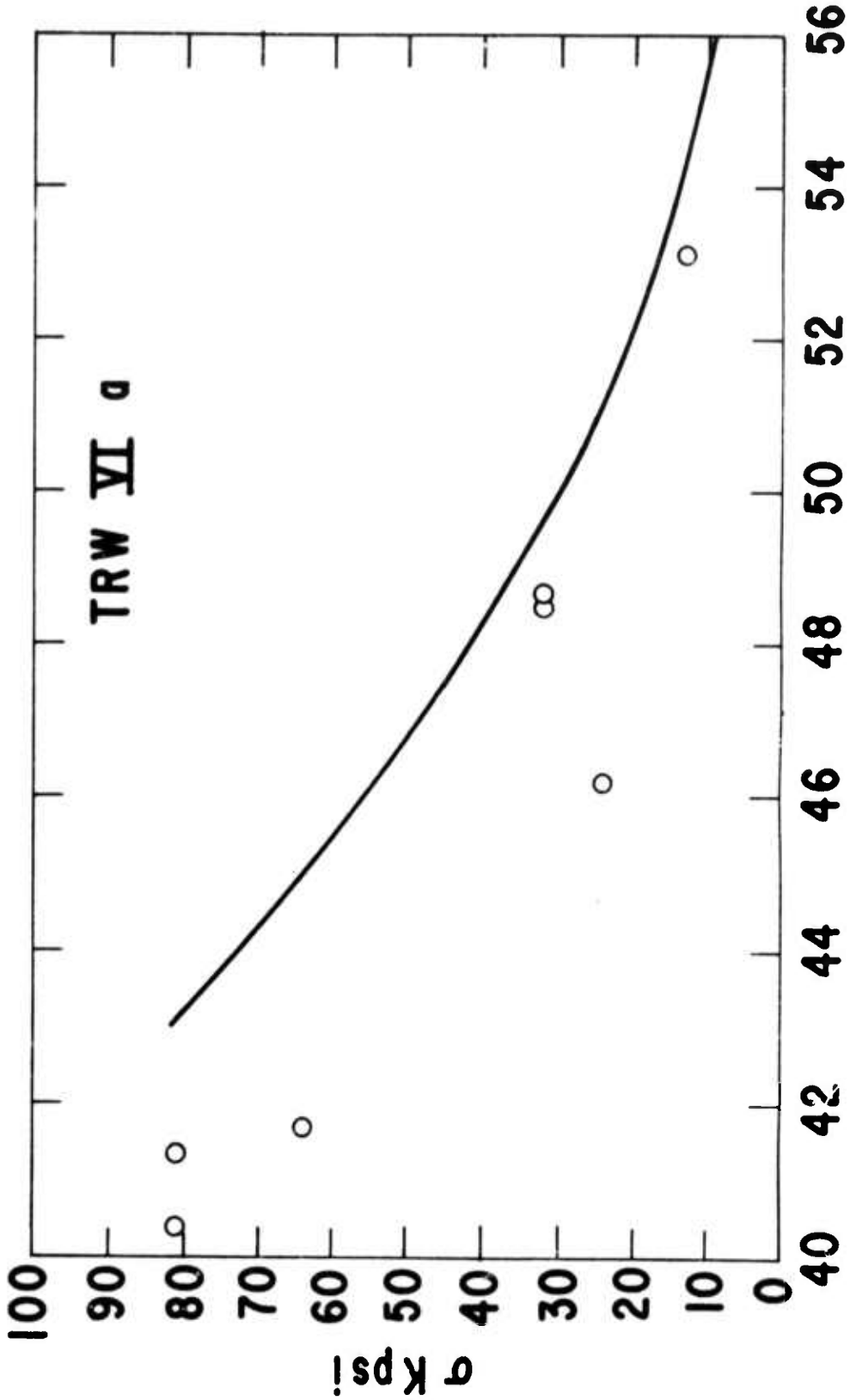

Figure 44. Stress rupture properties of permanent mold cast TRW VI A.

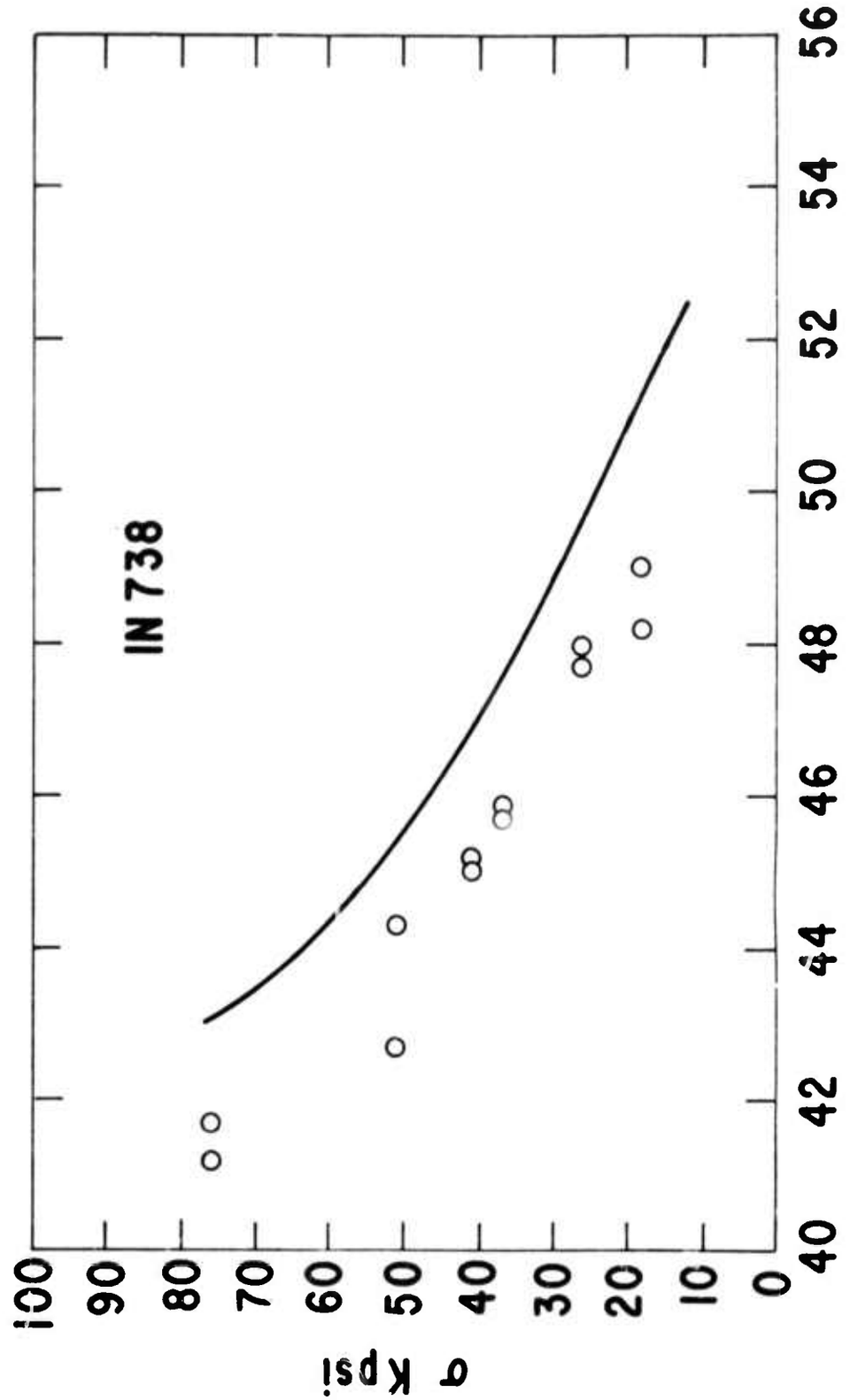

Figure 45. Stress rupture properties of permanent mold cast IN 738.

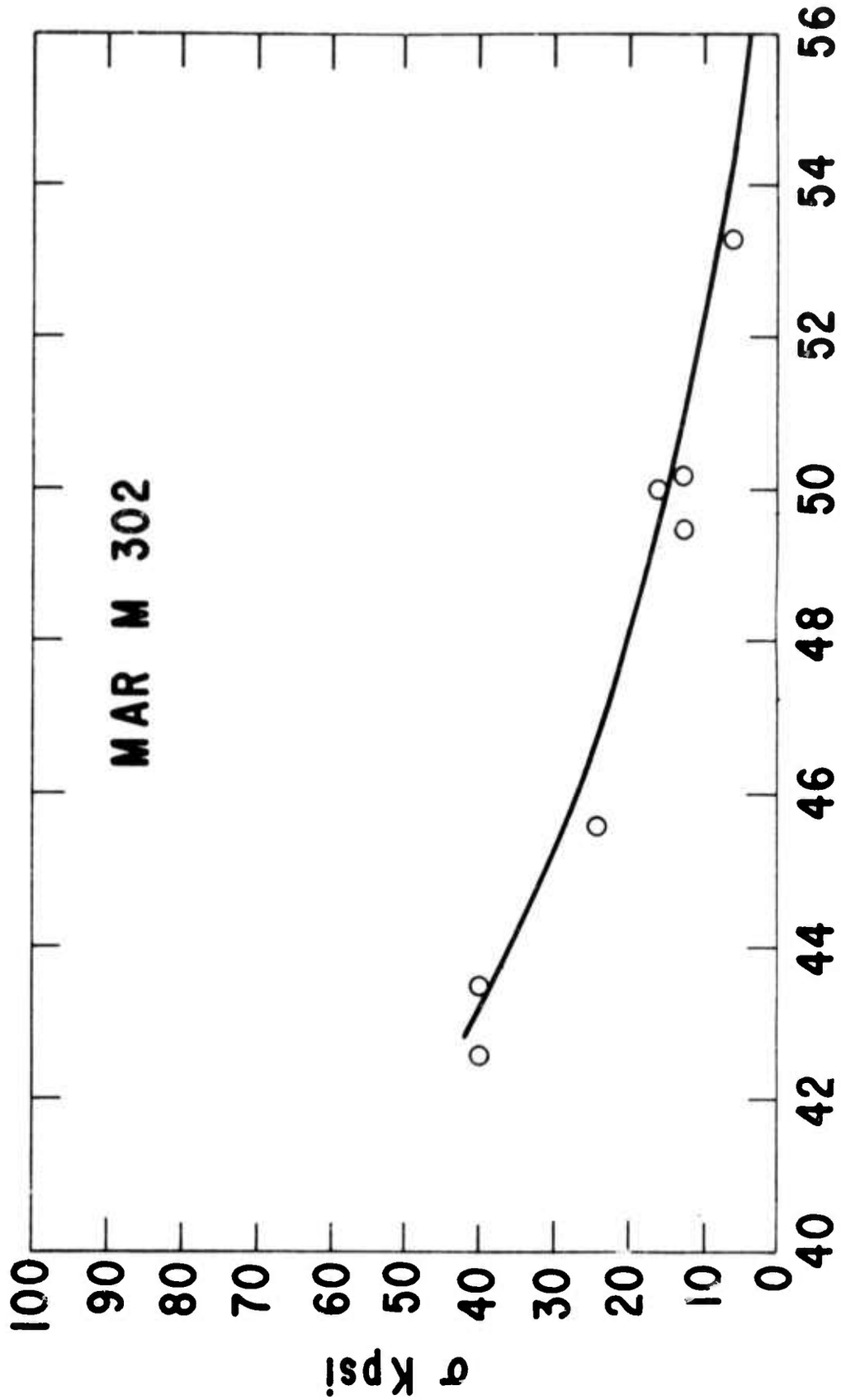

Figure 46. Stress rupture properties of permanent mold cast Mar M 302.

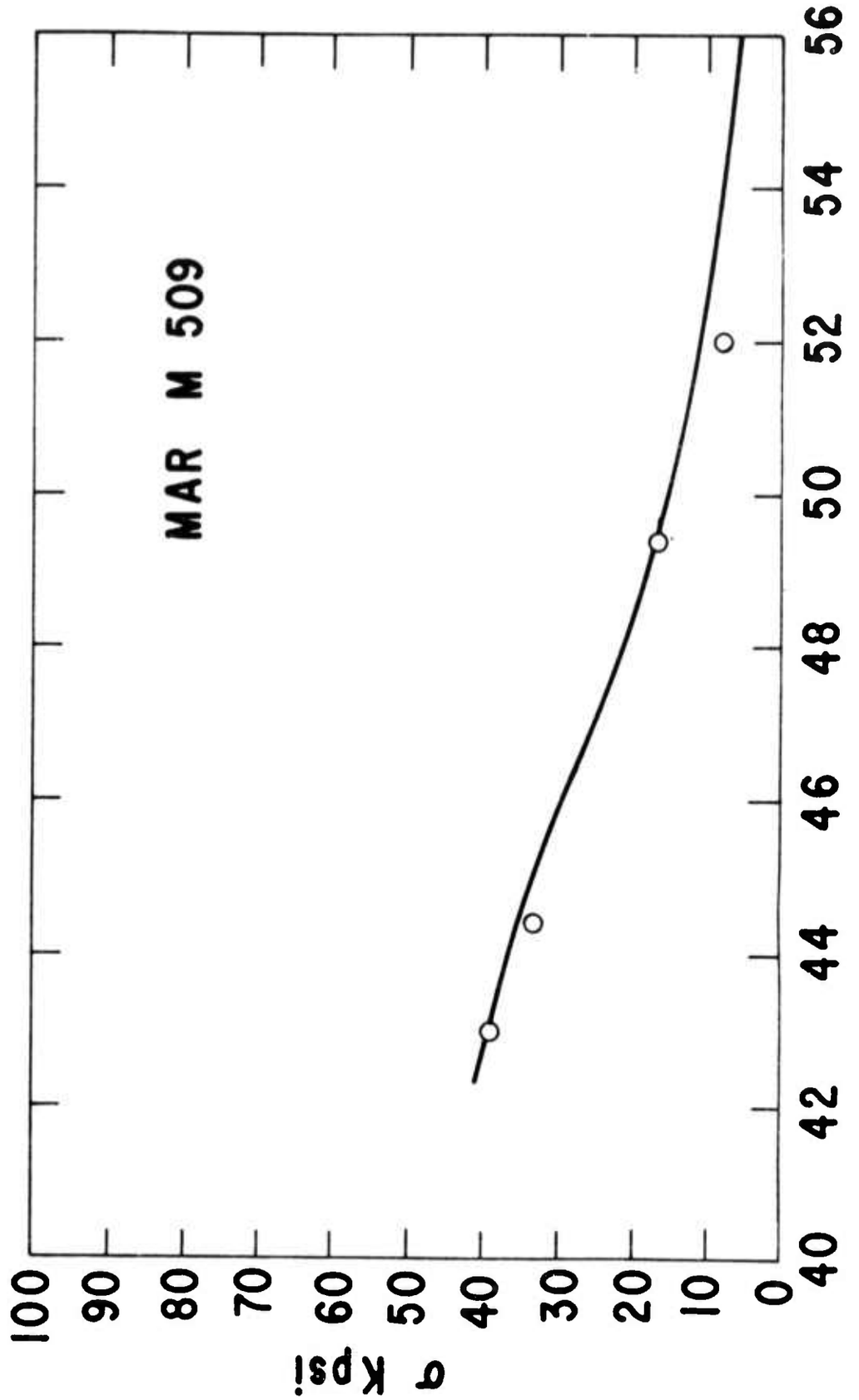

Figure 47. Stress rupture properties of permanent mold cast Mar M 509.

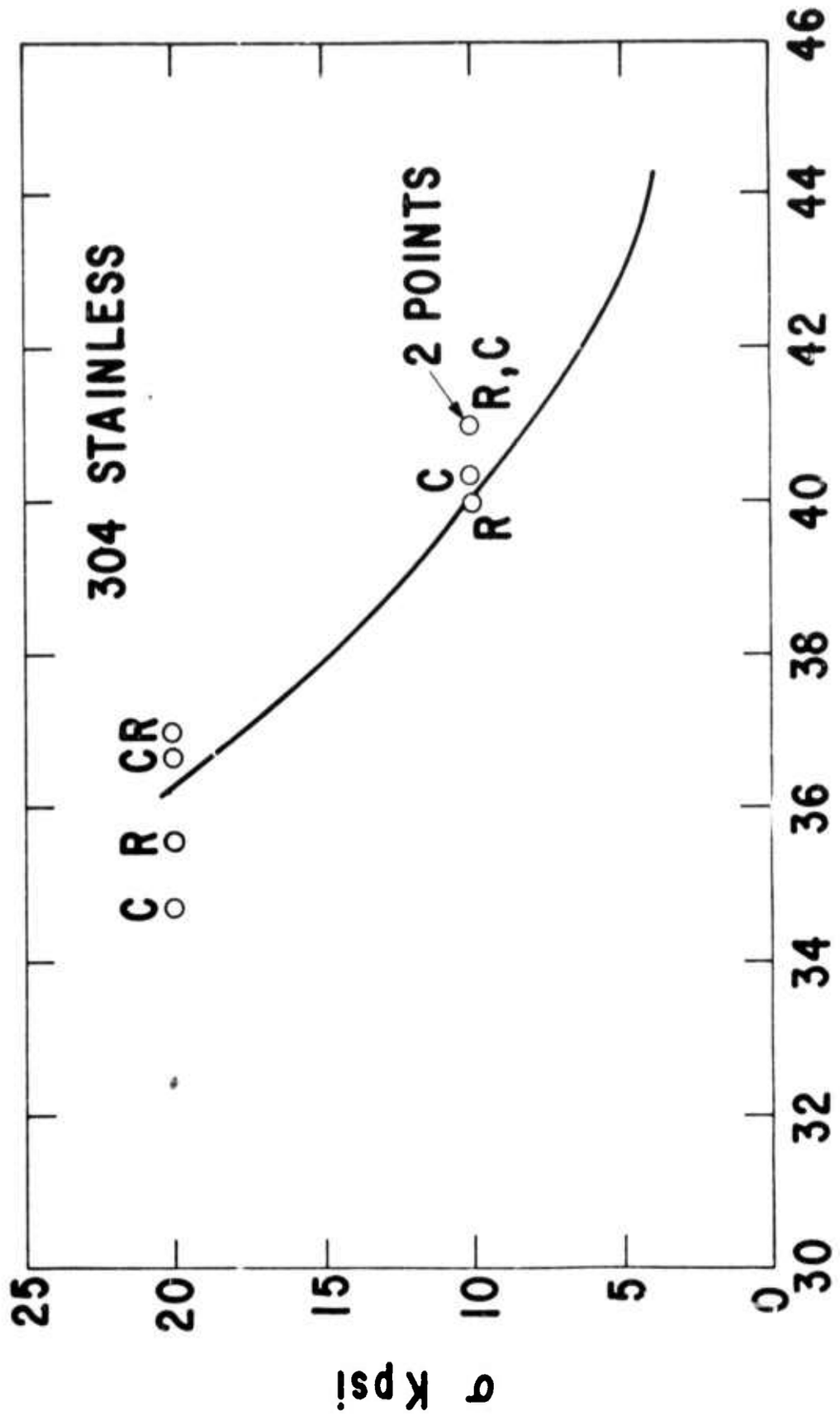

Figure 48. Stress rupture properties of conventional and rheocast 304 stainless steel.

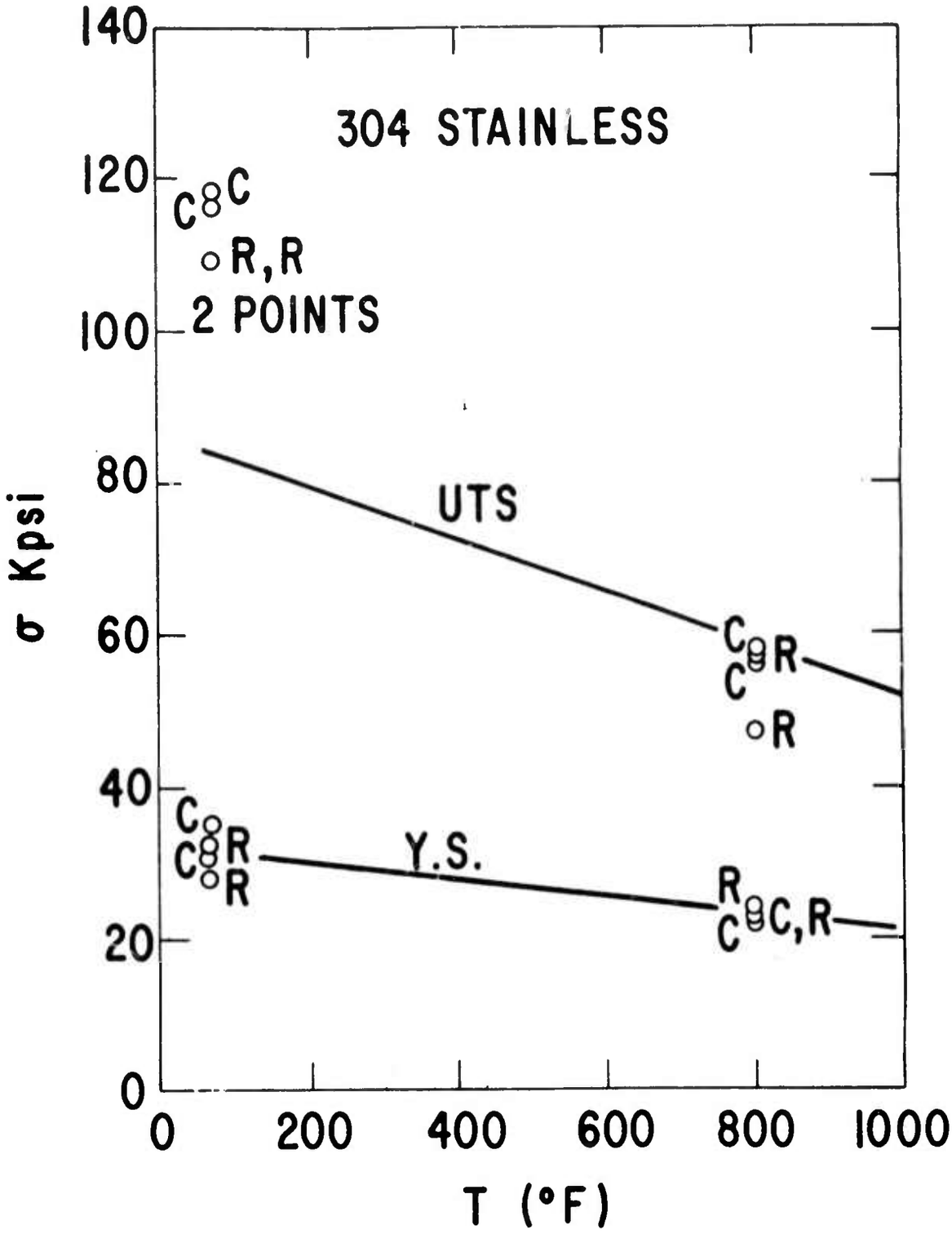

Figure 49. Tensile properties of conventional and rheocast 304 stainless steel.

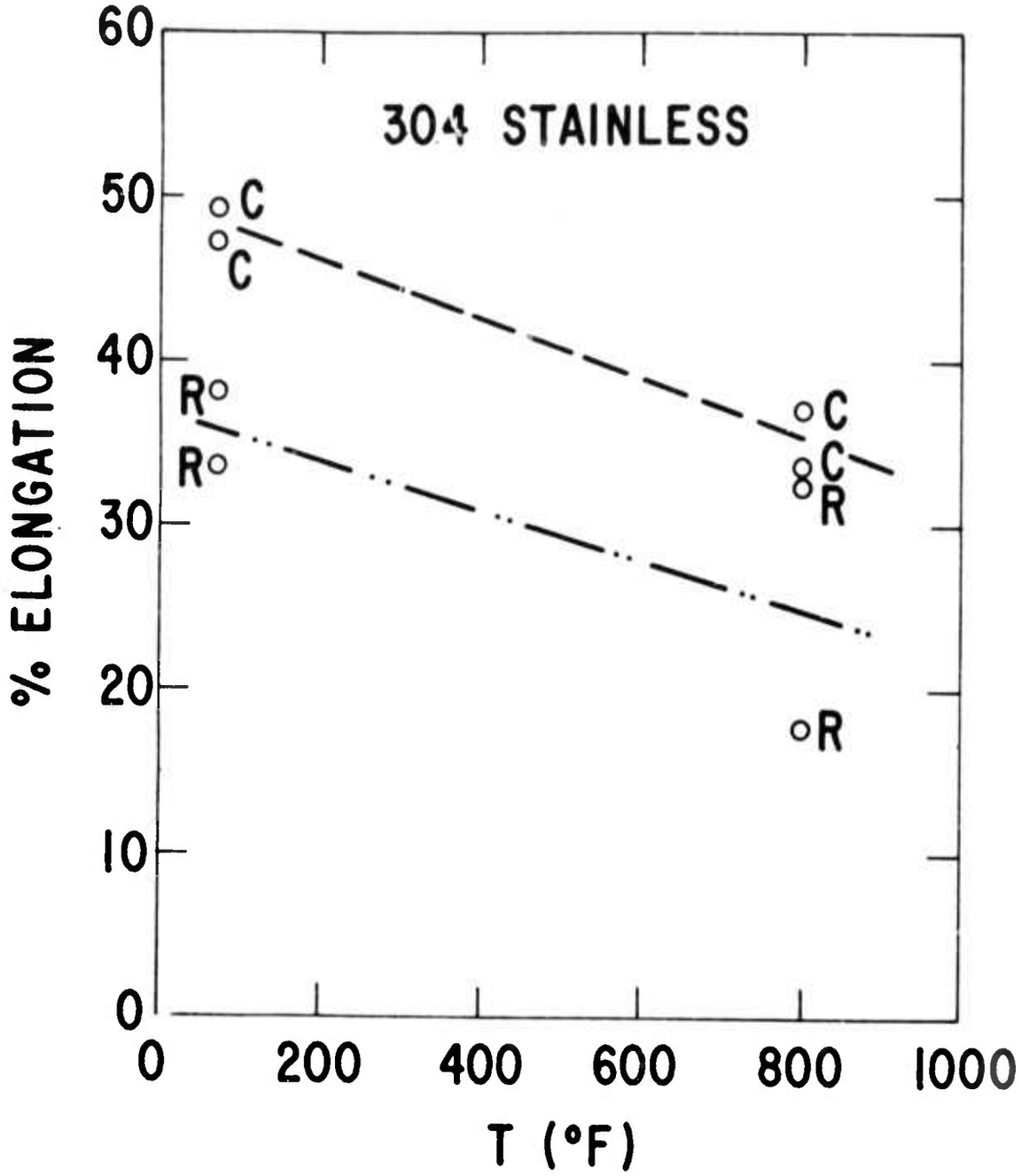

Figure 50. Tensile ductility of conventional and rheocast 304 stainless steel.

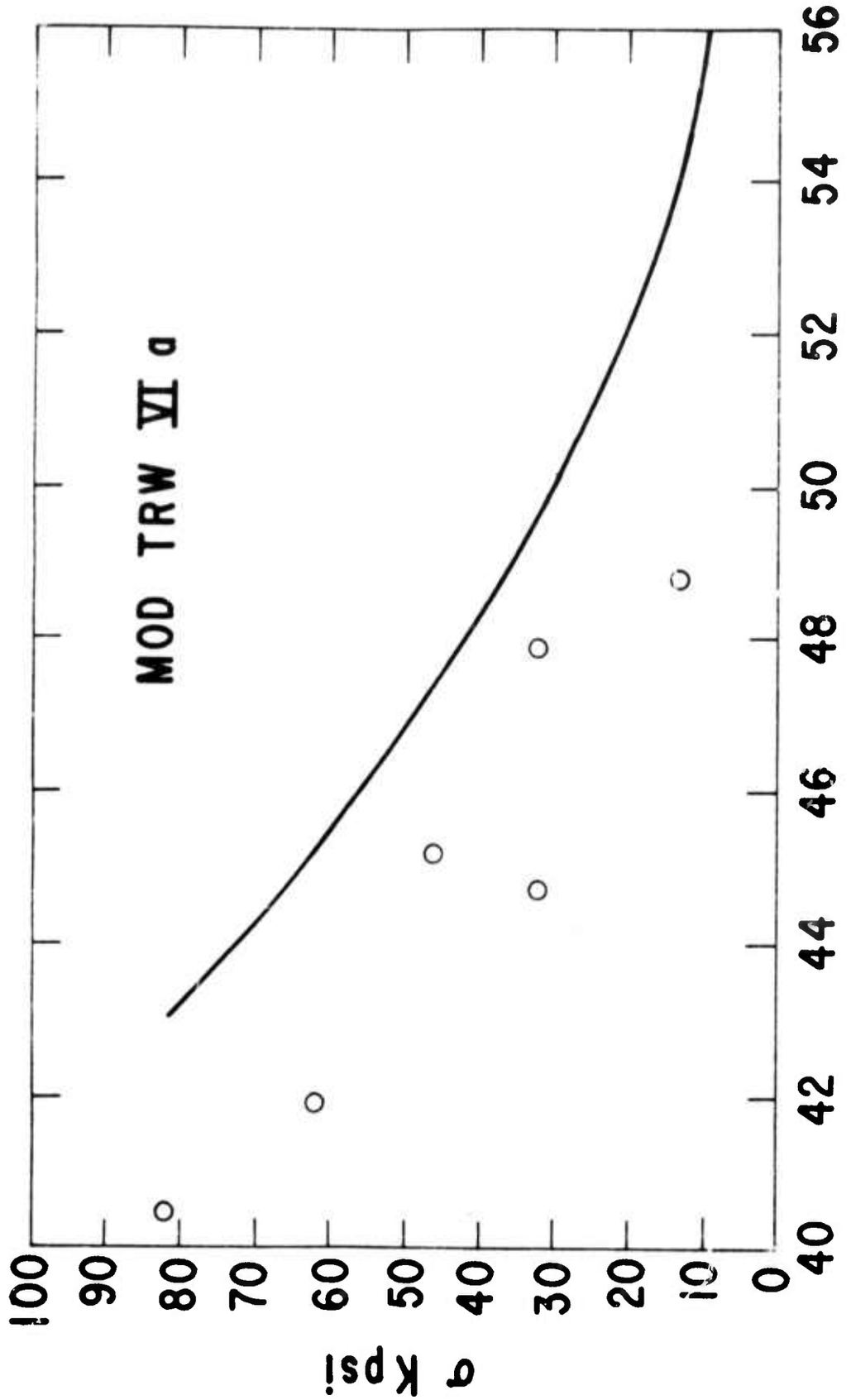

Figure 51. Stress rupture properties of modified TRW VI A.

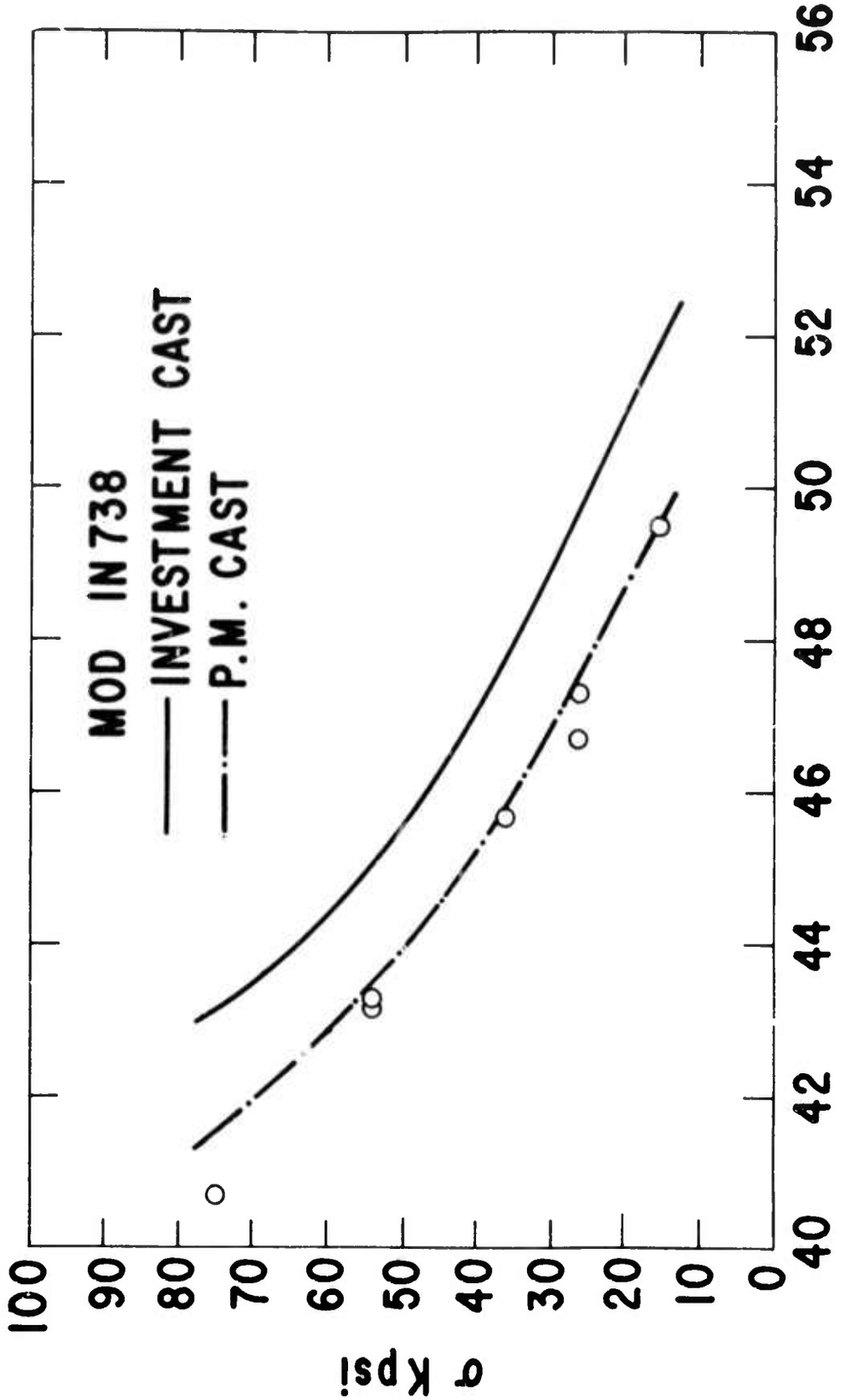

Figure 52. Stress rupture properties of modified IN 738. Properties are similar to the permanent mold cast.

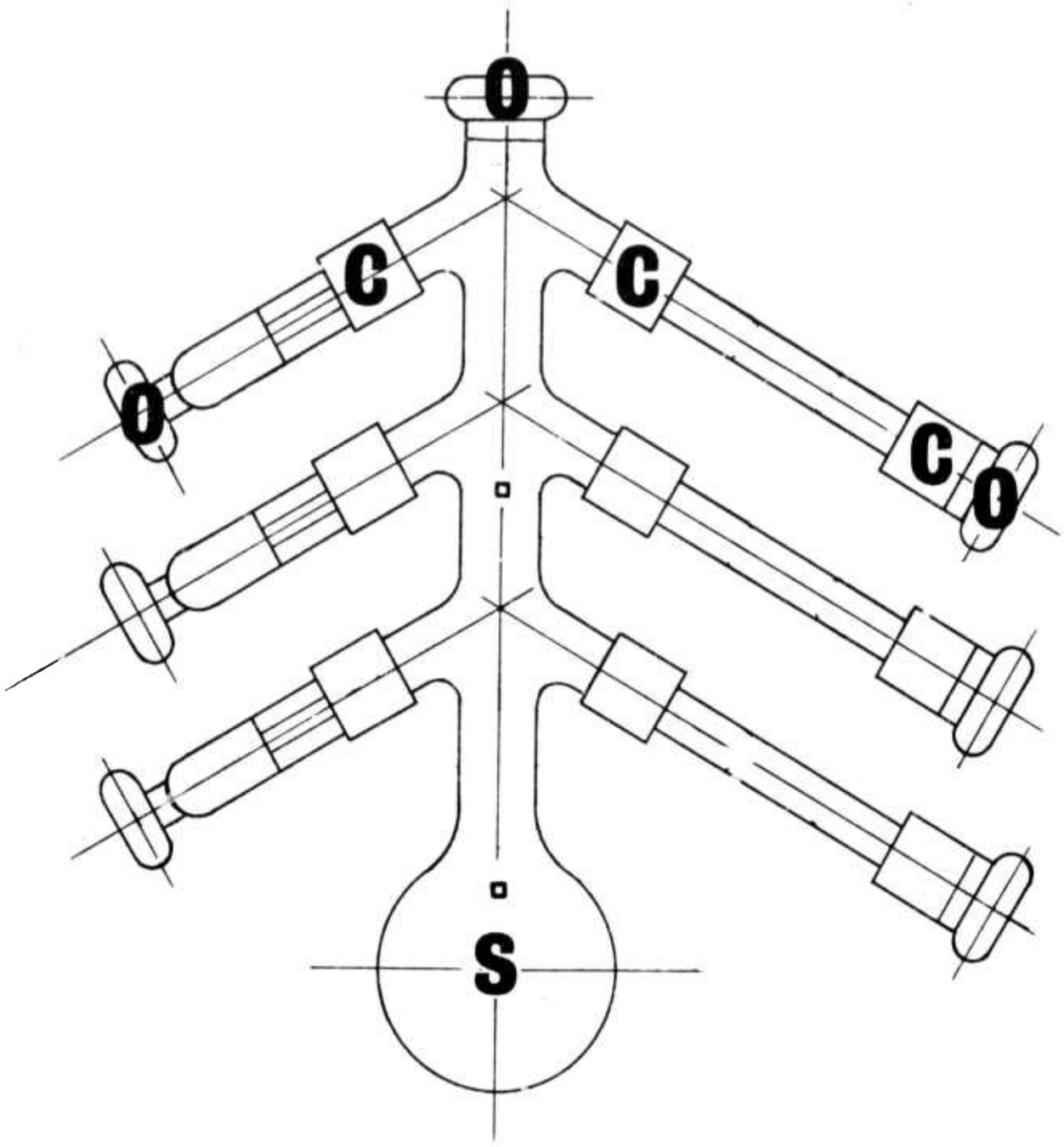

Figure 53. Die insert design showing positions of ceramic insert risers C, over flow and vents O, and shot sleeve S.

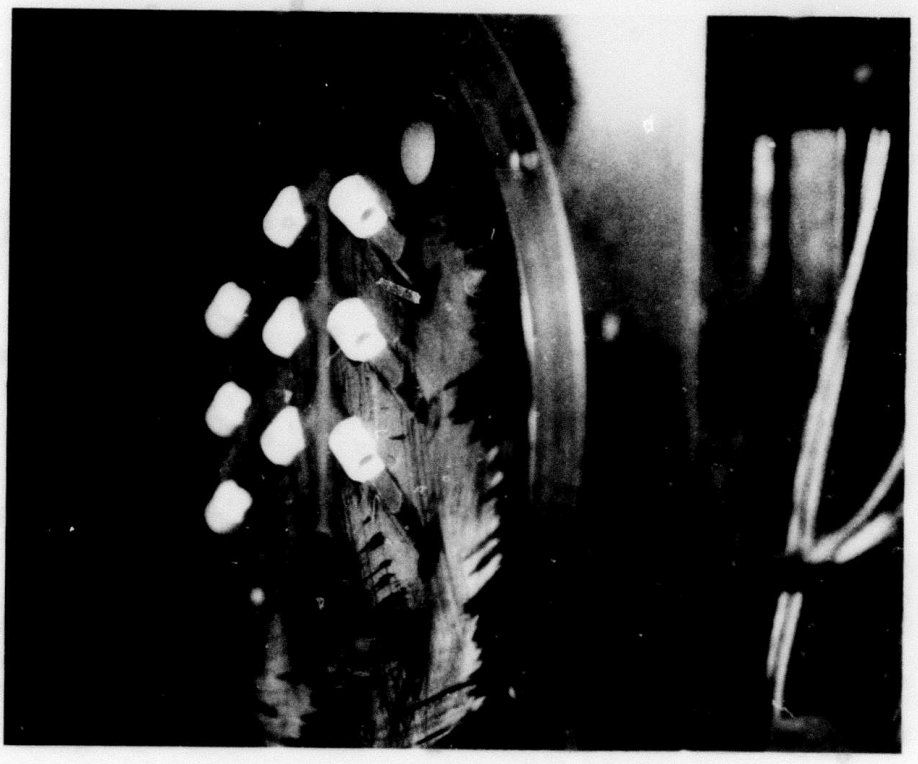

Figure 54. Die insert installed in die set.

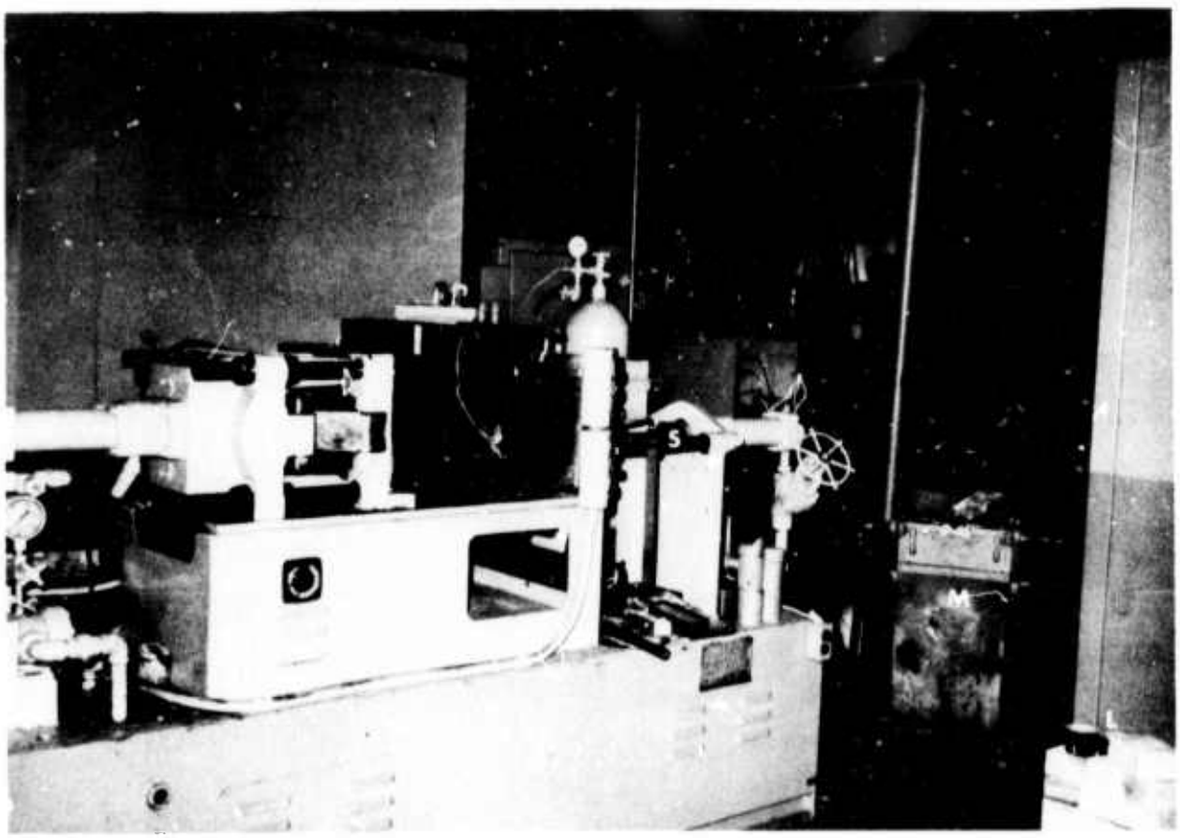

Figure 55. Die casting machine. Shot sleeve at S, melt furnace at M, ladle preheat at L.

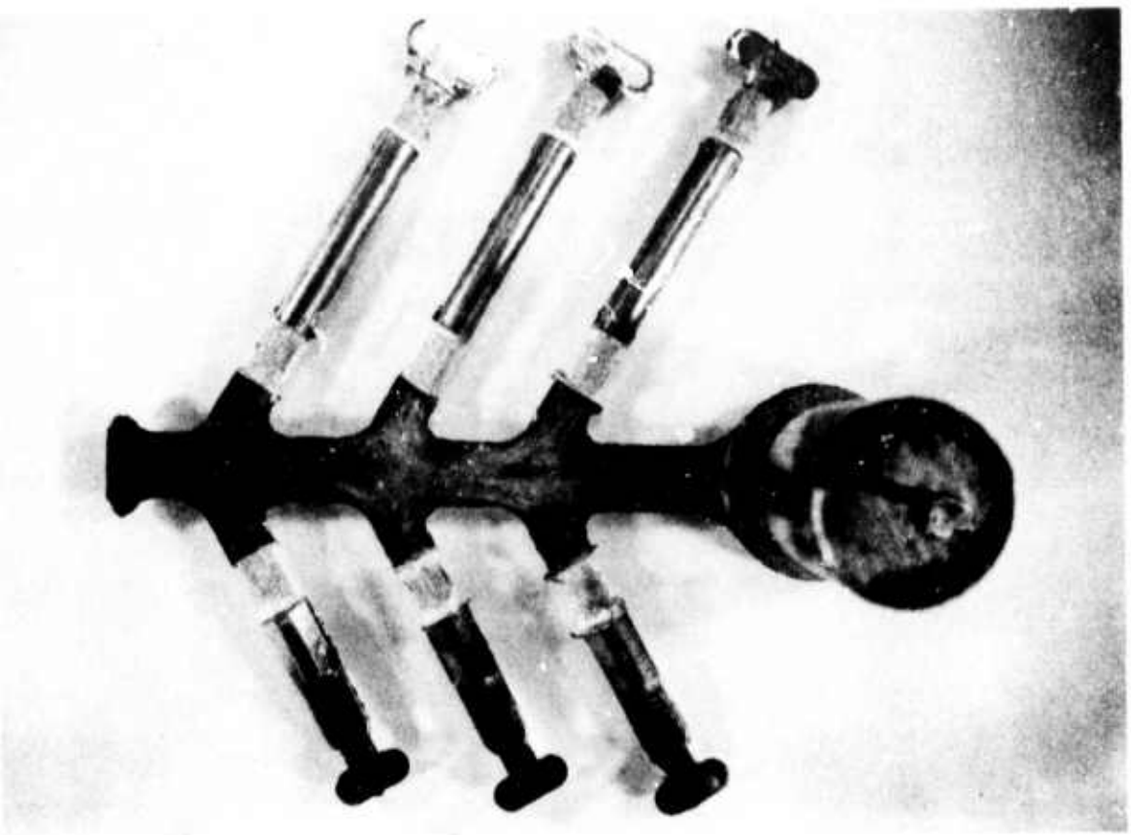

Figure 56. Aluminum die casting top surface. Risers removed.

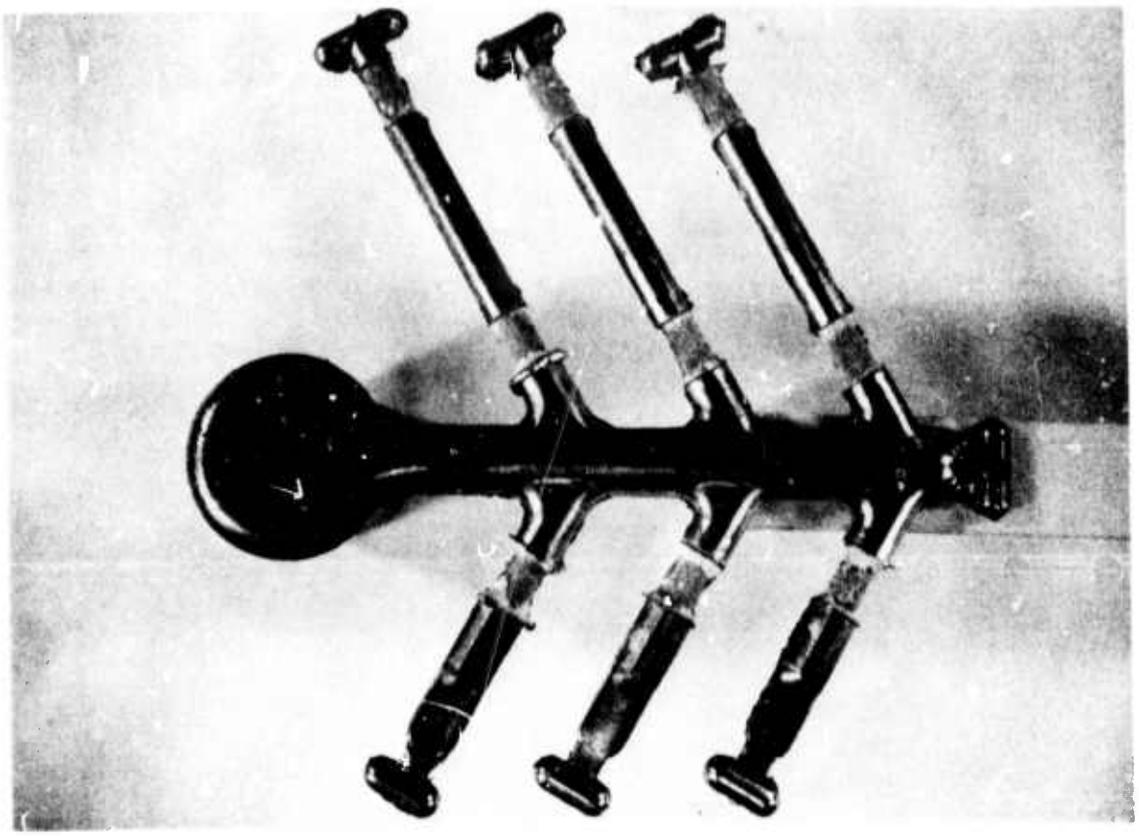

Figure 57. Aluminum die casting bottom surface. Risers removed.

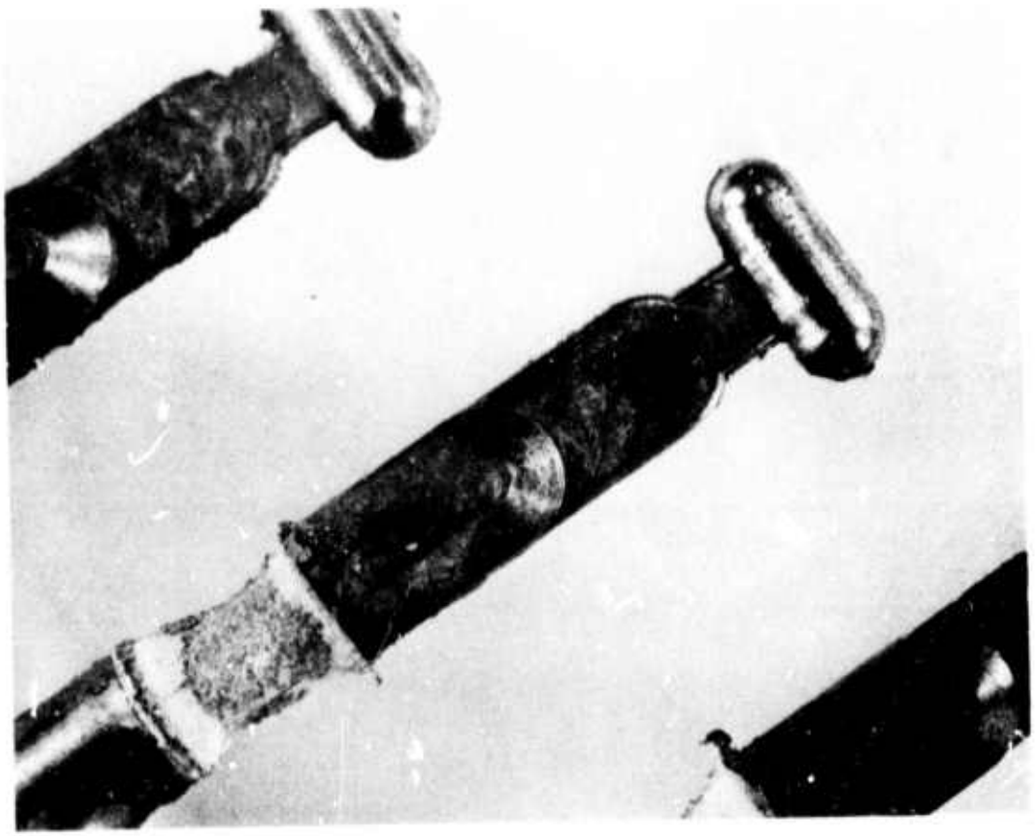

Figure 58. Detail of aluminum die casting.

Figure 59. Stainless steel die casting. 34°C superheat. Ceramic risers in place.

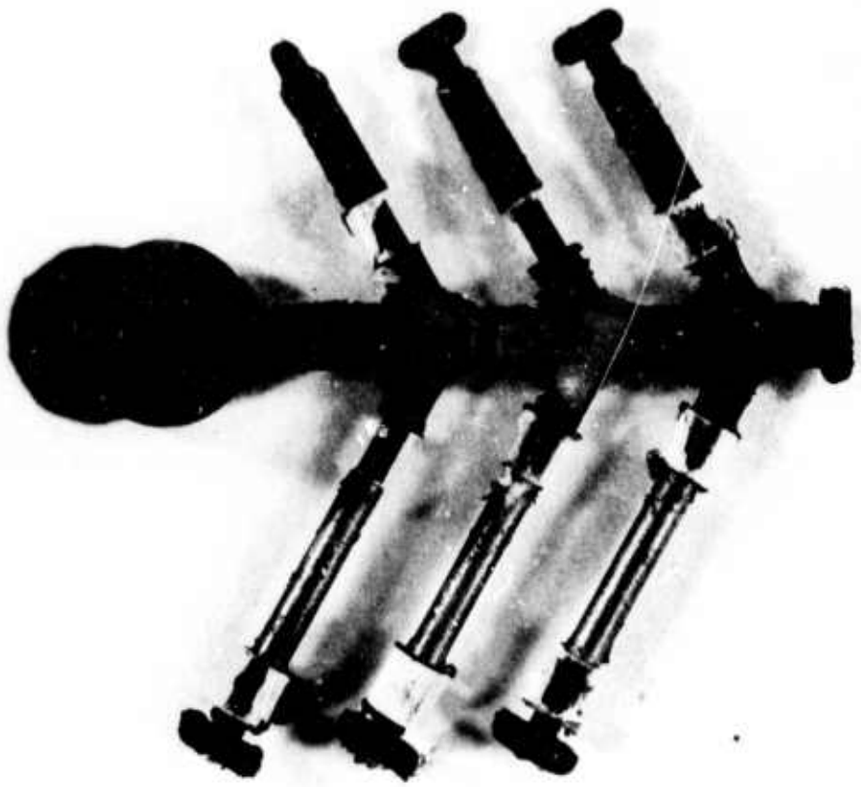

Figure 60. Stainless steel die casting. 102°C superheat. Ceramic risers in place.

Figure 61. Stainless steel die casting. 105°C superheat. Cu inserts in place.

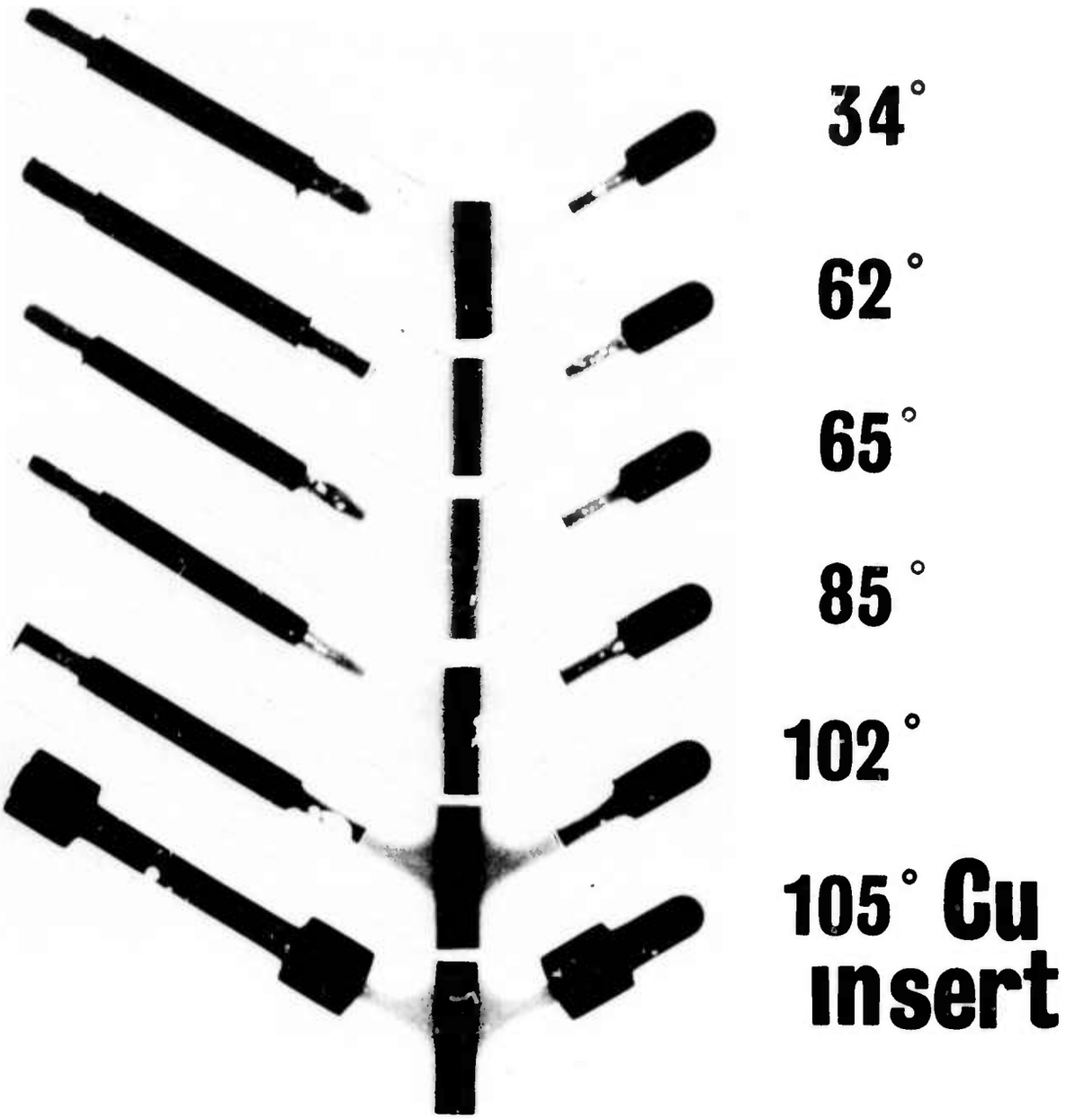

Figure 62. X-ray photographs of the bar from stainless steel die castings as a function of superheat.

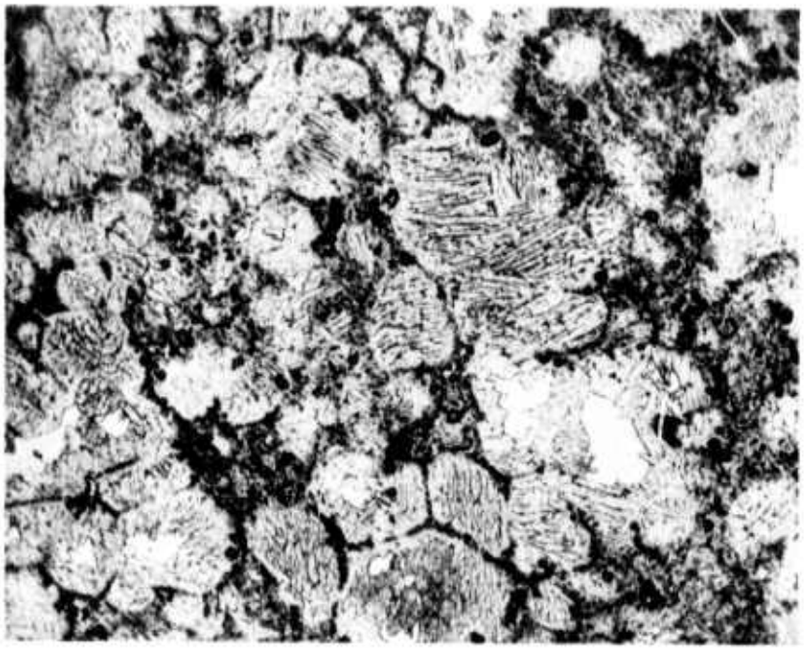

Figure 63. Microstructure of 304 stainless die casting. 65°C superheat. 250X.